

Spring 2018

UAV-BASED GEOTECHNICAL MODELING AND MAPPING OF AN INACCESSIBLE UNDERGROUND SITE

Elizabeth Anne Russell
Montana Tech

Follow this and additional works at: https://digitalcommons.mtech.edu/grad_rsch



Part of the [Geological Engineering Commons](#), and the [Geology Commons](#)

Recommended Citation

Russell, Elizabeth Anne, "UAV-BASED GEOTECHNICAL MODELING AND MAPPING OF AN INACCESSIBLE UNDERGROUND SITE" (2018). *Graduate Theses & Non-Theses*. 177.
https://digitalcommons.mtech.edu/grad_rsch/177

This Thesis is brought to you for free and open access by the Student Scholarship at Digital Commons @ Montana Tech. It has been accepted for inclusion in Graduate Theses & Non-Theses by an authorized administrator of Digital Commons @ Montana Tech. For more information, please contact sjuskiewicz@mtech.edu.

UAV-BASED GEOTECHNICAL MODELING AND MAPPING OF AN
INACCESSIBLE UNDERGROUND SITE

by

Elizabeth Anne Russell

A thesis submitted in partial fulfillment of the
requirements for the degree of

Master of Science in Geoscience:
Geological Engineering Option

Montana Tech

2018



Abstract

Digital photogrammetry is becoming a more common method used for mapping geological and structural rock mass features in underground mining. The issue of capturing geological and structural data in inaccessible, unsupported areas of mines remains even when utilizing terrestrial photogrammetric methods; thus, geotechnical models of mines are left with incomplete datasets. Large unsupported underground voids, like stopes, have the potential to cause major failures, but by filling in the geotechnical data gaps in inaccessible areas, potential failures can be predicted through kinematic analysis of the area's mapped discontinuities. Implementation of Unmanned Aerial Vehicles (UAVs) in underground mines and recent advances in obstacle detection systems have allowed for greater experimentation with photogrammetry conducted from a UAV platform in mines.

For this study, a UAV-based underground photogrammetry system was developed to manually capture imagery in an inaccessible stope at Barrick Gold Corporation's Golden Sunlight Mine (GSM) in Whitehall, Montana, to see whether or not the approach is a viable remote sensing technique for gathering georeferenced geotechnical data. Development of the system involved selecting an appropriate UAV platform, identifying a lighting system capable of providing adequate illumination, acquiring a sensor system that consistently avoids obstacles, and choosing the appropriate UAV camera (and its respective settings) for underground UAV-based imaging. In order to georeference the data collected in the inaccessible stope, paintballs were shot into the stope to create ground control points that were then surveyed in laser range detection. These paintball marks had to be in visual line-of-sight and visible in the imagery captured via UAV camera in order to georeference them.

Using the imagery collected in the stope at GSM, models were constructed and structural features were mapped on those models. Bentley ContextCapture software was able to successfully construct a stope model from the video frame imagery collected via UAV in the stope, while ADAM Technology was not. Split-Engineering's Split-FX and ADAM Technology were used separately to map the discontinuity planes present within the model. A comparison of underground discontinuity mapping was performed using the UAV-based photogrammetry captured in the stope and hand mapping data collected around the entrance to the stope. It was found that northeasterly striking discontinuity planes were identified using the digital mapping, but not in hand mapping. Using UAV-based photogrammetry for geotechnical data collection creates a quick and thorough mapping process with time-stamped imagery that can potentially create a safer mine. The lessons learned during this study may help guide future efforts using UAVs to capture geologic data and to help monitor stability in areas that are inaccessible.

Keywords: UAV, photogrammetry, geotechnical, inaccessible, underground, model

Acknowledgements

My great appreciation is extended to Mary MacLaughlin and Ryan Turner for playing a huge role in the writing of the grants that have funded this project and my last year of school. I would like to thank the Geological Engineering department as well for trusting me as the first Graduate Research Assistant funded through the department. I would like to offer my special thanks to all of the students on the UAV team for their continual assistance and support throughout the project, including Jay Hillygus, Jack Fitzgerald, Rachel Becker, Liana Galayda, Cooper Knoll, Ninad Bhagwat and Charlie Linney. Additionally, I am grateful for my committee members, Larry Smith and Jeremy Crowley, who continually challenged me to learn more about the UAV industry and were patient with all of my thesis edits. Also, I would like to thank Nick Barney, of Montana Tech, who continually fought through all of my repeated software battles.

Barrick Gold Corporation's Golden Sunlight Mine (GSM) and underground contractor Redpath Mining employees, especially Sean Chabot, Clint Mortenson, and Brian Dale, helped to make this project possible by providing a safe site for conducting fieldwork. GSM helped to make our survey possible by providing the equipment, as well.

This material in this document is based upon work supported by the National Science Foundation under Grant No. CMMI-1742880, and by the Alpha Foundation for the Improvement of Mine Safety and Health under Grant No. AFC518-67. The views, opinions and recommendations expressed herein are solely those of the author and do not imply any endorsement by the National Science Foundation or the ALPHA FOUNDATION, their Directors and staff. Some financial support was also provided by Montana Tech.

Table of Contents

ABSTRACT	II
ACKNOWLEDGEMENTS	III
LIST OF TABLES.....	VII
LIST OF FIGURES.....	VIII
GLOSSARY OF TERMS	XII
1. INTRODUCTION	1
2. OVERVIEW OF MAPPING AND MODELING TECHNIQUES.....	4
2.1. <i>Traditional Techniques</i>	6
2.2. <i>Remote Sensing Techniques</i>	8
3. PROPOSED RESEARCH	14
3.1. <i>Research Objectives</i>	14
3.2. <i>Research Approach</i>	16
3.3. <i>Data Collection Site</i>	17
4. UAV SYSTEMS	20
4.1. <i>DJI Phantom 4 Pro</i>	20
4.2. <i>DJI Matrice 100</i>	21
4.2.1. Camera	22
4.2.2. DJI Guidance System	22
4.2.3. On-board Lighting Systems.....	26
5. UAV FLIGHTS: PREPARATION, TESTING, AND DATA COLLECTION	28
5.1. <i>P4P and Associated Systems Testing</i>	29
5.2. <i>M100 and Associated Systems Testing</i>	31
5.2.1. DJI Guidance System Testing	32
5.2.2. On-board Lighting Systems Testing	34

5.2.3.	UAV/Remote Controller Communication Testing	39
5.3.	<i>Georeferencing Technique Testing</i>	39
6.	UNDERGROUND DATA COLLECTION	42
6.1.	<i>Flight in the 815-102 Drift</i>	42
6.2.	<i>Flight in the NEV Stope</i>	44
7.	MAPPING AND MODELING SOFTWARE AND RESULTS	47
7.1.	<i>ADAM Technology Software Approach</i>	48
7.2.	<i>ContextCapture and Split-FX Software Approach</i>	49
7.3.	<i>Modeling and Mapping the 815-102 Drift as a Proof-of-Concept</i>	50
7.4.	<i>Results from the NEV Stope</i>	53
8.	CONCLUSIONS AND RECOMMENDATIONS	62
9.	REFERENCES CITED	68
10.	APPENDIX A: UAV SYSTEMS	75
10.1.	<i>DJI Phantom 4 Pro</i>	75
10.1.1.	Compasses and IMUs	75
10.1.2.	Flight Modes	76
10.1.3.	Camera	76
10.1.4.	Obstacle Sensing and Avoidance	77
10.1.5.	On-board Lighting Systems	79
10.2.	<i>DJI Matrice 100</i>	80
10.2.1.	Compass and IMU	81
10.2.2.	Flight Modes	81
10.2.3.	Camera	82
10.2.4.	DJI Guidance System	83
10.2.5.	On-board Lighting Systems	83
11.	APPENDIX B: FLIGHT PROCEDURES	86
11.1.	<i>Calibrating the Compasses and IMUs</i>	86
11.2.	<i>Calibrating the DJI Guidance System</i>	87

11.3.	<i>Indoor Flights</i>	88
11.4.	<i>Outdoor Flights</i>	89
11.5.	<i>Underground Flights</i>	89
12.	APPENDIX C: WORKFLOW AND PROCEDURES	92
12.1.	<i>ADAM Technology Software</i>	92
12.2.	<i>Bentley ContextCapture Software</i>	93

List of Tables

Table I. Lighting control test combinations used underground at GSM and corresponding image quality	36
Table II. Measured Lux values from a controlled test of the four lighting systems considered for use on the M100.....	37
Table III. Ground control points (GCPs) that were measured in drawpoint 1 of the NEV stope using the Trimble Total Station and two known survey points. These values are in the local mine coordinate system.....	45

List of Figures

- Figure 1. Examples of field mapping techniques used for measuring discontinuities in a rock mass, including a scanline survey (*left*) and cell mapping (*right*) (modified, Mathis 1987)
6
- Figure 2. Diagram of sub-level open stoping in an underground mine (Atlas Copco, 2007).
18
- Figure 3. (*Top*) An example of one of the five sensors that use LED indicators to confirm if the Guidance system is being used for detecting obstacles through the DJI Guidance cameras and ultrasonic sensors (DJI GUIDANCE User Manual, 2015) and (*Bottom*) the DJI Guidance mounted to the bottom of the M100 UAV.23
- Figure 4. DJI Guidance sensor ranges and blind spots (*DJI GUIDANCE User Manual, 2015*).
24
- Figure 5. A screenshot of the warning that appears in the center of the connected mobile device screen when obstacles are being detected by the DJI Guidance system that is on-board the M100.25
- Figure 6. *Left*: Lume Cube and connector used for attaching Lume Cubes to M100, *Right*: Firehouse Technology Light and connector used for attaching the Firehouse Lights to the M100.26
- Figure 7. Photograph of the M100 underground photogrammetry set-up with the Stratus LED 100W LED Modules (circled) attached on adjacent arms.27
- Figure 8. Photos of (*Left*) an out of LOS flight with P4P in the basement of the MG building and (*Right*) the P4P flight in UMEC where Tripod Mode was tested and terrestrial lighting was used to light the rock face.31

- Figure 9. Measured lux as a function of distance away from a rock face for the four different lighting systems for use on the M100 tested underground at GSM (Turner et al., 2018).
.....38
- Figure 10. Reflector installed on the mine rib at a known coordinate (on the local mine grid) that is used for determining the total station location by performing a resection.....40
- Figure 11. (*Left*) UAV team member shooting paintballs onto ribs for creating control points and, (*Right*) Control points created on the ribs in yellow (blue arrows are pointing to paintball marks). For scale the height of the paintball gun operator in the image to the left is 1.7 m (5ft. 7in.) tall. In the photo to the right, the wire mesh has 25 mm (4 in.) spacing and the UAV (with the propeller guards) measures about 1.2 m (4 ft.) diagonally.41
- Figure 12. GSM’s ISite point cloud of the NEV Stope (modified, Brian Dale). For scale, the height of the drawpoints (in the vertical direction) is approximately 5 m (16 ft.).44
- Figure 13. A merged DTM (top) of one rib of the 815-102 drift at GSM created using ADAM Technology software with the plan view (bottom) of the drift to display the erroneously curved shape that the software produced. This model was constructed from UAV-based video stills.51
- Figure 14. The 815-102 drift rib mapped (and modeled) using ADAM Technology software with color coded structure orientation; some joints demonstrate erroneous orientations of structures that are in the same set in reality.51
- Figure 15. Bentley ContextCapture model built of the 815-102 drift rib at GSM. This model was constructed from the same UAV-based video stills as the model constructed in the ADAM Technology software.52

- Figure 16. Structures shown in purple and red that were identified and mapped using Split-FX on the ContextCapture model of the 815-102 drift rib at GSM.52
- Figure 17. Bentley ContextCapture 3D models of the NEV Stope at GSM created from UAV imagery; the top image shows a model made with 225 stills and the bottom image shows the model made using 446 stills all extracted from the video imagery. The yellow dots show the locations of the measured ground control points used for constructing the model. The red dot is a control point that was measured, but not used for constructing the model.55
- Figure 18. ContextCapture 3D stope model showing the camera locations (in white wireframe) in relation to the parts of the model that were captured and the parts that were not (the holes).56
- Figure 19. Two ContextCapture model tiles mapped using Split-FX: the location of some of the planes used for mapping the structures may not be located in the correct location on the model, but remain in the correct orientation due to a glitch within Split-FX.57
- Figure 20. ContextCapture model mapped using 3DM Analyst with structural planes present within the NEV Stope color-coded by orientation set.59
- Figure 21. Hand mapped structure present in the drift leading to the stope drawpoint entrance (top) and within the first drawpoint entrance (bottom) (GSM mapping files).60
- Figure 22. Stereonets (in equal area projection) of mapped joint sets in the NEV Stope and areas leading into the first drawpoint of the NEV Stope at GSM using Split-FX (left), 3DM Analyst (right), and hand mapping (bottom).61

Figure 23. DJI Phantom 4 Pro obstacle sensor locations (Phantom 4 Pro/Pro+ User Manual, 2017): rear [1], front [2], and downward [3] cameras used for positioning, downward ultrasonic sensor [4], and 3D infrared sensor [5].	78
Figure 24. Ranges of obstacle detection sensors and associated blind spots on the DJI Phantom 4 Pro (DJI Phantom 4 Pro/Pro+ User Manual, 2017).	79
Figure 25. <i>Left</i> : Lume Cube lights attached to P4P for testing, <i>Right</i> : Firehouse Technology lights used for testing on-board the P4P.	80
Figure 26. Before (<i>left</i>) and after (<i>right</i>) photos of one of the automobile drain plugs that was machined to create customized UAV leg connectors for the M100.	85
Figure 27. UAV compass calibration diagram showing the positions of the rotational axes and directions in which the system must be rotated for the calibration to be successful (DJI Matrice 100 User Manual, 2017).	87
Figure 28. General workflow for 3DM CalibCam project (Lingen, 2011).	93
Figure 29. General workflow for constructing a photogrammetry model in Bentley ContextCapture (Bentley, 2018).	94

Glossary of Terms

Term	Definition
Back	in underground metal mining, the top or roof of the tunnel (drift)
Drift	in mining, an underground opening usually constructed at set dimensions that allows for access to ore; also used for mining ore; a tunnel constructed for underground mining
Rib	in underground metal mining, the side walls of the tunnel (drift)
Sill	in underground metal mining, the floor or base of the tunnel (drift)

1. Introduction

Remote sensing techniques are commonly used to capture data for geotechnical analyses and have become a reliable source for gathering structural mapping data (Vallejo and Ferrer, 2011; Lato and Vöge, 2012). Oftentimes, geological data can be collected through these same techniques as well. By utilizing remote sensing techniques, geotechnical engineers are able to define structural orientations of rock mass discontinuities and create software-ready inputs for analyses (Levy and Visca, 2009). Routinely, remote sensing techniques are used to capture data from large areas that would take much more time to gather without the remote sensing aid. These techniques are beneficial because they capture time-stamped data notably in areas that are “unknown” in terms of the structural geology (Coggan et al., 2007). In the underground mining industry, the gaps in knowledge of the structural data, especially in inaccessible areas of mines, often create significant potential for danger (Azhari et al., 2017).

Photogrammetry is an advantageous remote sensing tool used for mapping and modeling, especially in areas that cannot be reached or accessed safely by humans (Kottenstette, 2005; Coggan et al., 2007). Safety concerns, lack of the appropriate equipment, a need for more detailed mapping, a limited budget, and time constraints are all basis for implementing photogrammetric techniques in place of traditional mapping (Dang, 2015; Coggan et al. 2007). In utilizing this remote imagery process, three-dimensional (3D) models are built for conducting quantitative analyses, especially for geotechnical characterization (Levy and Visca, 2009). Although the terms “mapping” and “modeling” are often used interchangeably, in the context of this study, “modeling” refers to the rendering of a 3D model of the rock mass geometry and “mapping” refers to geologic and structural orientation measurements taken from the model (e.g. the strike and dip of a joint). If traditional techniques like field mapping are used for collecting

geotechnical information, the data often have to be manually digitized into a usable format that can be used in or imported into a software package for analysis and for application to other on-site design processes (Levy and Visca, 2009). Digital photogrammetry allows for the mapped geotechnical features to be exported into workable forms for analysis and application in other software (Kottenstette, 2005).

Other geotechnical remote sensing techniques are able to capture structural data in underground environments as well, but often do not provide RGB (red green blue) color imagery data useful for identifying geologic boundaries. For example, laser scanner systems can provide 3D point cloud data for identifying rock mass geometries, but the systems require supplemental photos to be taken, separately, for modeling RGB color data on the point cloud (Levy and Visca, 2009; Liu, 2013). Alternatively, photogrammetry provides an all-in-one solution by capturing structural data and imagery in one process. A point cloud created using photogrammetry inherently has RGB values projected onto each point showing the true color of the object (Liu, 2013). With current technological advancements in digital cameras, photogrammetry progressively yields higher quality and more edifying outputs for identifying structures in 3D models of rock masses.

Today, Unmanned Aerial Vehicles (UAVs) with on-board digital cameras are employed for remote sensing data capture techniques for inspections, vegetation analyses, volumetric calculations, comparative studies based on changes over time, project progression monitoring, assessing slope stability, and other applications (Coggan et al., 2007; Remondino et al., 2011; Birch, 2009; Greenwood et al., 2016). UAV-based photogrammetry is becoming more prevalent as UAVs, UAV-specific cameras, and photogrammetric software become more affordable and user-friendly (Greenwood et al., 2016). Using a UAV-based photogrammetric platform enables

fast data collection, especially in areas that cannot be accessed safely by humans (Remondino et al., 2011). In addition, photogrammetric software have become more geared toward integrating UAV-based imagery, versus carefully planned terrestrial photos as in the past.

In the geotechnical realm of mining, UAVs have been used for geologic site reconnaissance and to assess slope stability, measure structure, and map geologic features within the rock masses (above and below ground) in areas of concern (Tamburini et al., 2015; Greenwood et al., 2016). As technology has advanced, 3D geologic models and their inherent applications in industry have advanced with high resolution data captured at faster speeds (Colomina and Molina, 2014). Additionally, with more research on obstacle detection sensors, especially in the industry of autonomy (i.e. self-driving cars), sensors have evolved to be more finely tuned and to effectively sense and avoid objects that are in the sensor's path. Advancements in obstacle avoidance sensors and UAV-based cameras create the potential to utilize off-the-shelf UAVs for mapping inaccessible areas that are not visible to the UAV operator.

The objective of this study is to assess the viability of using UAV-based imagery and photogrammetry to model and map rock masses that are inaccessible in underground mines. To achieve this objective several components must be considered, including: capturing UAV-based digital imagery with the appropriate lighting and settings, flying the UAV without crashing by using an obstacle detection system, creating 3D digital photogrammetry models from video frame stills, and mapping discontinuity features within the digital model. The overall goal is to provide a safer and more efficient method for characterizing rock masses in providing a more comprehensive dataset for future mine designs, support, and excavations.

2. Overview of Mapping and Modeling Techniques

Collecting geotechnical data at an underground mine site is important for conducting rock mechanics analyses and for understanding the rock masses. Traditional techniques, like cell mapping and scan line surveys, are commonly combined with remote sensing techniques for characterizing the rock masses being excavated at mine sites. Underground mines create a more challenging and limited geotechnical data collection scenario than do surface mines; there is usually less rock exposure available within underground excavations, and there are areas that cannot be accessed or seen due to safety concerns. The inability to access the rock mass creates data gaps where the rock has been excavated, and may be left unsupported. Using photogrammetry as a remote sensing technique for modeling these inaccessible areas, via UAV-based imagery, helps to fill these gaps in geotechnical knowledge. In combining the current knowledge of the project's underground site with the photogrammetric data, a more complete understanding of the mechanical and geologic properties of the rock masses, especially in inaccessible areas, can be achieved.

Mapping geology and geologic structure is a critical factor in designing underground mining excavations (Hoek, 2007). Knowledge of geomechanical rock parameters allows a geotechnical engineer to assess potential modes of structural failure in the rock mass. Geotechnical data capture techniques provide insight into the rock mass type, strength, and stresses while taking hydrogeological conditions into consideration, so that the properties of the rock mass can be understood.

Quality indices based on qualitative and quantitative field observations have been developed for geomechanical classification of rock mass strength (Vallejo and Ferrer, 2011), and may be used for estimating rock mass strength (failure criteria e.g. Mohr-Coulomb or Hoek-

Brown criterion). These failure criterion estimations generally involve the assumption that the rock mass is isotropic, which is rarely the case (Hoek et al., 1995). Rather, the rock is usually intersected by different types of discontinuities, including bedding planes, faults, joints, and foliation. Discontinuity orientations are usually measured by cell mapping or conducting a scanline survey. Rock mass quality indices typically provide the most representative estimates of rock mass strength (Vallejo and Ferrer, 2011).

The limited ability to collect data from within the rock mass and lack of exposed rock surfaces create a large gap in knowledge, which is exacerbated in active areas of an underground mine where the rock is inaccessible, making mapping impossible. Traditional mapping techniques such as field mapping (sometimes combined with using one or more quality indices) and core logging can be time consuming when employed for collecting detailed structural data (Liu, 2013; Vallejo and Ferrer, 2011). As a result, traditional geotechnical mapping techniques are often combined with faster remote sensing techniques, yet not all above-ground remote sensing techniques can be implemented for use underground. One of the major limitations in capturing data beneath earth's surface is that geospatial positioning and satellite imaging cannot aid in underground data collection. Global navigation satellite systems (GNSSs) like GPS (global positioning systems), cannot penetrate the ground surface (Zlot and Bosse, 2014). Many remote sensing techniques are dependent upon GNSS; thus, underground geotechnical remote sensing techniques are limited to technologies such as photogrammetry (or imagery) and laser-based systems including light detection and ranging (LiDAR) and simultaneous localization and mapping (SLAM) systems (Lato and Vöge, 2012; Delaloye et al., 2012; Liu and Kieffer, 2012; Zlot and Bosse, 2014). Both the traditional and remote sensing data collection techniques have associated limitations.

2.1. Traditional Techniques

Traditionally, hand mapping and borehole core logging have been the principal techniques utilized for determining geologic boundaries and structural features of underground rock masses (Hoek et al., 1995). Borehole core logging and surface outcrop mapping are regularly performed prior to mining. Core can be used for laboratory testing, generally in preliminary design stages, to determine the rock mass properties and in-situ stresses associated with each rock type. Field mapping, also referred to as hand mapping, commonly consists of identifying lithologies, geologic contacts, and geologic structure, including the orientation of discontinuity planes within a rock mass. Cell mapping consists of measuring structural orientations within a representative “cell” – a marked area of the rock face (Mathis, 1987). The number of joints per joint set and the number of joints with one end in the window and both ends in the window may be recorded in cell mapping to estimate discontinuity length. The spacing between the joints may be measured by the number of fractures crossing the imaginary horizontal centerline of the cell. For scanline surveys, a baseline above the ground surface is identified and a measuring tape is stretched across the rock. Joints extending above the tape are mapped and their location is recorded. Diagrams showing examples of a scanline survey and a cell map are illustrated in Figure 1.



Figure 1. Examples of field mapping techniques used for measuring discontinuities in a rock mass, including a scanline survey (*left*) and cell mapping (*right*) (modified, Mathis 1987)

Core logging and hand mapping can be expedited when necessary, but require significant time for conducting detailed mapping used to estimate geological and structural properties used for support design (Vallejo and Ferrer, 2011). In addition to the core logging and surface mapping, regional maps of the geology and geophysical studies are used for collecting geotechnical information about the site in the early stages of mining as well (Hoek et al., 1995).

As mining progresses, field mapping can be carried out in underground openings to collect geotechnical data to understand the rock strength, deformability, and quality for more insight into the geomechanical properties of the rock mass for support design (Vallejo and Ferrer, 2011). Today, the most commonly used rock mass classification systems are the Rock Mass Rating Quality Index (RMR), and the Rock Tunneling Quality Index (Q) (Hoek et al., 1995; Vallejo and Ferrer, 2011). Both RMR and Q are empirical methods developed to help estimate the strength and deformability parameters of rock masses and predict the behaviors of the rock masses (Vallejo and Ferrer, 2011), and are applied through field observations and measurements of the intact rock and discontinuity parameters. Q and RMR produce a quantitative value for the quality of the rock mass (Hoek, 2007). Q incorporates the block size formed by the rock joints, the shear strength between those blocks, and the influence of the state of stress experienced by the rock mass (Vallejo and Ferrer, 2011). RMR classifies structural regions of the rock mass using the uniaxial compressive strength of the rock, rock quality designation (RQD), discontinuity characteristics, and groundwater conditions (Hoek, 2007). RQD is integrated into both quality indexes. It is a quantitative measurement of the degree of fracturing within a rock mass – essentially the percentage of core that is recovered in “long” pieces. RQD determinations can be made using drilled core and/or observations of rock exposures, whether in outcrop or an underground production face. The Geological Strength

Index, GSI, is another index applied for determining the strength properties of a rock mass. Compared to RMR and Q, GSI is a more qualitative classification system commonly applied to poor or very poor quality rock masses (Vallejo and Ferrer, 2011). It is based on the geological, structural, and alteration parameters observed in the rock mass without including any measurements of laboratory values or RQD. All of these traditional systems, however, tend to overestimate the geomechanical properties of rock masses through their respective oversimplification of a heterogeneous rock mass with varying conditions (Vallejo and Ferrer, 2011). With an increasing understanding of the rock mass and its surrounding conditions throughout the mining process, these indices are modified to each specific site (Hoek, 2007).

2.2. Remote Sensing Techniques

In recent decades, two primary remote sensing techniques have been used for underground geotechnical modeling and mapping: laser-based systems and digital photogrammetry. Both produce a point cloud, a 3D mesh, and a 3D surface on which geologic structures can be mapped. Laser-based systems produce a point cloud of the structure that is within line-of-sight (LOS) of the system (Coggan et al., 2007). From the point cloud, a mesh is made by connecting the points to form triangles or rectangles, and a respective surface is formed by infilling those triangles or rectangles. The laser-based systems used for underground data collection include terrestrial laser scanners or LiDAR and SLAM. The terms LiDAR and laser scanner can be used interchangeably. LiDAR emits laser pulses (at a constant speed) onto a target and measures the elapsed time or the phase shift of the reflected pulse, depending upon the system (Levy and Visca, 2009; Delaloye et al., 2012). The time or phase shift is used to determine the distance between the system and the target. If corresponding images are available of the area, they can be overlain onto the point cloud surface. SLAM uses a set of algorithms or

software to simultaneously locate itself while modeling in real-time (Haines, 2016). The SLAM system can be a laser-based system or visual based (using imagery). Commonly, SLAM uses lasers for point cloud generation when used in dark environments, like underground mines. Photogrammetry, on the other hand, uses photographs to create a 3D scene (Birch, 2006). Digital photogrammetry does not overlay the imagery onto the point cloud as laser scanning does; instead, photogrammetry uses 2D coordinates from stereo pairs (overlapping 2D images) to determine 3D coordinates of match points in the imagery. The match points are locations captured in two or more photos that have been identified to exist at the same 3D location in space. To refine the visual reconstruction of the 3D model, digital photogrammetry software performs a bundle adjustment of the 3D coordinates (Birch, 2009).

Typically, the underground mining industry has favored laser scanning over digital photogrammetry because it does not require an external light source (Azhari et al., 2017). Laser scanning allows for a more streamlined and convenient methodology for collecting the geometry data needed to create a 3D model, because it is not as site specific as photogrammetry. For different sites, separate camera lenses, lens calibrations, lighting systems, and imagery settings must be considered. Drawbacks in laser scanning include time for data collection and equipment expenses (Donovan and Lebaron, 2009; Coggan et al., 2007). Also, photogrammetry has often captured joint sets that laser scanners have previously missed (Donovan and Lebaron, 2009). Otoo et al. (2011) states that when used alone, LiDAR scanning cannot measure traces, which are joints that extend perpendicular into the rock face with minimal dilation.

Laser-based systems, like LiDAR and SLAM, may have the ability to produce denser point clouds or build a 3D map while collecting data, respectively; however, those systems do not provide RGB values that can be projected onto each of the points in the point cloud, as

photogrammetry does. The closer the laser-based system is to the target being captured and the more lasers being used, the denser the point cloud. A study conducted by Delaloye et al. (2012) determined that repeated terrestrial LiDAR surveys could be used for tunnel deformation monitoring, specifically for circular openings. Deformation monitoring is important for assessing stability of the rock mass. Structural measurements of joints were not collected in the study, because the focus was on fitting Terzaghi's mean deformation ellipse (1942) to a deformed tunnel excavation. However, Liu and Kieffer (2012) successfully mapped discontinuities of an underground mine drift using data collected from a terrestrial LiDAR system and digital photography. The resulting geometry of the excavation was accurate to the millimeter scale. Recently, LiDAR has been tested by Emesent Autonomy via UAV platform in underground mining environments (personal communication, Dr. Stefan Hrabar, February 19, 2018). The LiDAR system was placed on a UAV and was autonomously flown down a mine drift and into a stope while scanning the drift shape. No record of mapped structural data has yet been released, although mapping the structural orientation of underground rock cuts using LiDAR data has been proven successful in multiple studies. For example, Lato and Vöge (2012) and Otoo et al. (2011) used built-in optical imaging on the LiDAR as an aid for mapping. Imagery was used in conjunction with the LiDAR point cloud to improve measurements of discontinuity orientations, in each case study mentioned previously. If imagery is necessary for mapping using LiDAR, then photogrammetry allows for one less data collection step in that the point cloud is created by the overlapping images.

On the other hand, documentation on the applicability of SLAM being used for mapping discontinuities underground was not found. Rather, the documentation detailed SLAM was used for collecting the geometric shape of underground drifts, efficiently. A SLAM system operates

using its real-time laser based (or imagery based) point cloud to locate its position while modeling continuously along the trajectory path (Zlot and Bosse, 2014); thus, a registered 3D map is created by the time the data collection is completed. Wu (2017) performed an experiment at Cortez Mine's Range Front Decline in Nevada, where he used a hand-held SLAM unit called GeoSLAM to model the structure of a drift while walking through it. No attempt was made to map this model, as its intended use was for efficient and accurate surveying and comparison with the mine design. The modeled geometry of the drift matched closely with that of the mine plan, proving the GeoSLAM to be a quick and accurate modeling tool. Prior to the handheld SLAM system experiment, a vehicle-mounted mobile SLAM unit was used for reconstructing an underground mine called Northparkes Mine in Goonumbla, NSW Australia (Zlot and Bosse, 2014). The 2D spinning laser scanning unit was mounted on the back of a vehicle and driven through approximately 17 km (over 10 miles) of the mine. The associated processing software automatically produced a point cloud from the scan. Although geotechnical data were not collected from the point clouds in these two studies, they do demonstrate the quickly advancing industry where laser scanning techniques are being used for collecting quick and accurate 3D surfaces. SLAM currently provides efficient modeling of underground drifts, but does not provide the level of detail necessary for measuring structural orientations of discontinuity planes in the model created.

To date, photogrammetry projects have been successfully conducted in underground environments (Gaich et al., 2007; Styles et al., 2010; Rees, 2012; Gaich et al., 2015). Gaich et al. (2007) used photogrammetry to create a blasting report of each drift blast, by making difference models between each model. The study conducted by Styles et al. (2010) looked at natural and stress induced fractures of an underground pillar by assessing the importance of rock bridges

using photogrammetry. Later, Rees (2012) confirmed that structural orientations and lithological contacts can be mapped using photogrammetric models in an underground mine. A few years after, photography captured while mounted on a tunnel boring machine was used to make a 3D photogrammetry model for characterizing rock mass geometries, for measuring joint spacing and orientations, and to map the geology in an underground mine (Gaich et al., 2015). Over the past 10 years, underground photogrammetry has progressed from simple terrestrial imagery, to imagery collected via a moving platform.

Recently, UAVs have been successfully flown underground, for modeling voids (Azhari et al., 2017). In the Azhari et al. (2017) study, UAV-based photogrammetry was successfully used in conjunction with SONAR to capture data and build a 3D photogrammetric model. The SONAR data were used to construct a baseline flight path of the void, which then allowed for successful collection of the high-resolution photogrammetry data needed to build the model. From the standpoint of UAV-based data collection, photographic methods of capturing data provide a more portable, inexpensive, and customizable substitute to laser scanners.

Donovan and Lebaron (2009) have claimed that photogrammetric methods are much faster than field mapping. In addition, Coggan et al. (2007) carried out a comparison of using laser scanning, photogrammetry, and hand mapping in which hand mapping proved to be the most time consuming techniques for collecting structural rock data. In the comparison, photogrammetry much more closely matched the hand mapped features as compared to those collected from the laser scanner data. Extensive photogrammetric research, both above and below ground, were conducted prior to the study in this current report (Coggan et al., 2007; Donovan and Ali, 2008; Donovan and Lebaron, 2009; Styles et al., 2010; Dang, 2015; Greenwood et al., 2016). These studies utilizing photogrammetry for characterization and/or

structural analyses of rock masses served as a baseline for formulating hypotheses for this research.

3. Proposed Research

Characterizing rock masses within and surrounding a mine plays a major role in designing support and assessing stability in that mine; thus, this research aims to assess the viability of using a UAV-based photogrammetry platform in underground inaccessible areas to capture imagery that can be used to create models and map geotechnical features. The model and mapped features will be compared using different software approaches. By collecting this data, a more complete database and a fuller understanding of geotechnical underground features can be achieved and allow for better prediction of rock fall and failures. In turn, this understanding and prediction of failure has the potential to foster a safer mining environment.

3.1. Research Objectives

The research conducted for this project supports efforts to establish UAV-based photogrammetry as a baseline technique for mapping rather than a supplement to field mapping. In order to be accepted as an adequate replacement for traditional field mapping, the data collected using UAV-based photogrammetry must be at least as accurate as data collected using traditional methods. With the rapid advancements in cameras, especially UAV cameras over the past few years, this goal is achievable. In order to successfully collect underground geotechnical data via a UAV-based photogrammetric system in inaccessible areas, four major questions had to be answered.

1. Can a UAV be flown out of LOS in an underground mine while remaining in connection to the remote controller?
2. Once out of LOS, will the UAV operator be able to keep the UAV in control, so that it does not crash and returns with the collected imagery?

3. Can the rock face be properly lit so that the imagery is sufficient for building a 3D model that can be used for geotechnical mapping?
4. How can a photogrammetric point cloud be georeferenced to create an accurate 3D model?

To prepare for flight in an inaccessible underground environment, many tests and practice flights were conducted. Below is a list of the activities undertaken prior to attempting to fly the UAV out of LOS flight in an underground stope:

- test indoor flying with obstacle avoidance system first with indoor lighting, then with only on-board lighting
- identify a lighting system that provides adequate light
- master indoor flight out of LOS
- determine whether data should be captured via video or photography
- test data capture settings underground to determine preferred settings for UAV data capture and 3D modeling/mapping
- stably fly UAV in underground mine (while simultaneously collecting UAV-based imagery and actively avoiding obstacles)
- test underground georeferencing techniques
- test underground UAV photogrammetry
- fly out of LOS in underground mine site
- successfully build and map a model using underground UAV imagery

After successfully conducting the list of activities, the first stope flight could be piloted with high probability that the UAV could be successfully flown out of LOS in an underground stope to collect imagery for building models and mapping orientations of discontinuities.

Successful flight includes stable flight control, active obstacle avoidance during flight, and the UAV's return to the operator with useable data. Achieving the four major research goals might contribute to engineering insight into areas that were previously unseen and unmapped and helping to create a safer mine by providing a better understanding of the possible ground stability hazards present in underground open voids. Through the success of this data-capture technique in stopes, other mining analyses like overbreak/underbreak assessments and ore body mapping could also possibly be achieved with the same system. Utilizing a UAV for photogrammetry in underground mining has potential to create a safer and more effective mining process.

3.2. Research Approach

Photogrammetry was selected as the remote sensing technique to be tested for mapping a large, inaccessible underground stope via the UAV platform because it is lightweight and affordable compared to laser-based techniques. In addition, using photogrammetry allows the geotechnical engineer to view and analyze a georeferenced, scaled model that creates a realistic surface with actual RGB color values collected through the imaging (Liu, 2013). The photogrammetry system was designed to utilize off-the-shelf type equipment capable of capturing structural data, such as discontinuities, in rock masses located in areas that are not safe to access in an underground mine. By analyzing structural data collected by the system, geotechnical engineers will have the potential to better predict fall-of-ground failures.

Because of the mercurial nature of the UAV market, UAVs were researched for months before the first was purchased. Criteria that the UAV had to meet included: customization with off-the-shelf sensor systems for obstacle avoidance, integration with a quality camera that could be used for underground photogrammetry, and capability to carry external lighting systems. The size of the UAV was taken into consideration, as well. The drifts at the selected research site,

Barrick Gold's Golden Sunlight Mine (GSM) in Whitehall, Montana, are approximately 5 m by 5 m (16 ft. by 16 ft.) (in height and width). With propellers included, the UAV systems that spanned over about 1.2 m (4 ft.) seemed "too large" for the available space. Also, it was recognized that the UAV would need to be a reasonable size for indoor practice flights in on-campus buildings and possibly other local facilities. To meet the project needs, the DJI Matrice 100 (M100) was selected as the main project platform. It was the only off-the-shelf system at the time that was found to have a sensor system that could be easily integrated with the UAV flight controller for obstacle detection and avoidance. The M100 was designed to be a more industrial and customizable UAV than other DJI UAVs that had been produced prior to the M100.

Two software approaches were taken for comparative modeling and mapping of the data collected: 1) ADAM Technology's 3DM CalibCam and 3DM Analyst were used for modeling and mapping, respectively, and 2) Bentley's ContextCapture used for modeling with Split Engineering's Split-FX used for mapping. First, the modeling/mapping systems were tested on an underground drift, for proof-of-concept and possible troubleshooting. Then, the data collected from a stope flight were used to create models and maps of the rock mass structure within the much larger and irregularly shaped stope. The digital discontinuity data from the 3D models were compared to hand mapping data collected around the entrance to the stope.

3.3. Data Collection Site

Data collection was carried out at GSM in Whitehall, Montana. GSM's underground mine, 2BUG, has implemented vein mining as well as sub-level longhole open stoping for recovering underground ore. Sublevel open stoping is a mining method involving sublevel drifts located above the main haulage road (Hamrin, 2001). The stope drilling is conducted from the

sublevel drifts, where ore is blasted in separate portions toward an open face. Once the ore is blasted, gravity causes the ore to pile at the bottom level at the drawpoints located along the haulage route where the ore is collected and transported to the mill for processing (Figure 2).

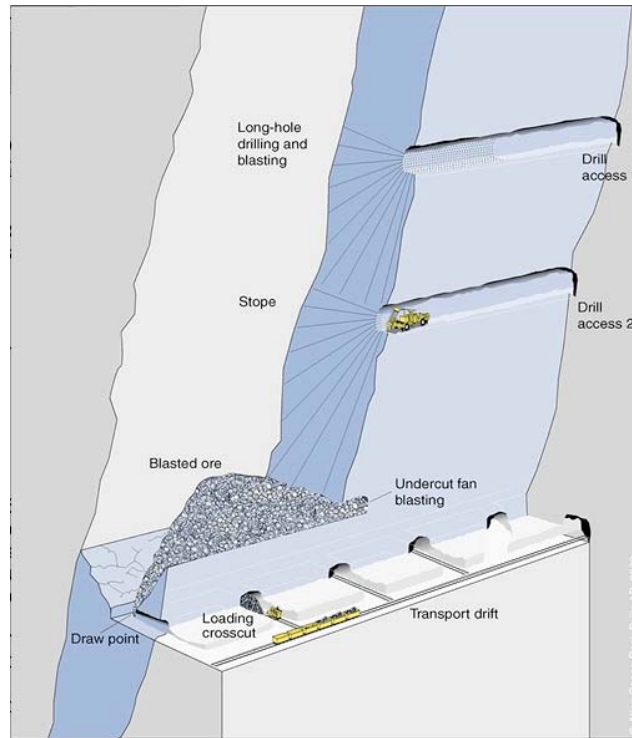


Figure 2. Diagram of sub-level open stopping in an underground mine (Atlas Copco, 2007).

Stopes at GSM can leave openings as large as 30 m (100 ft.) wide, 60 m (200 ft.) tall, and 60 m (200 ft.) long. Though the rock mass at GSM is fairly competent, rockfall incidents occur within the large, unsupported voids left from stoping that cannot be accessed by mine personnel; consequently, the geotechnical data necessary for predicting such failures of the stope rock mass cannot be collected using traditional mapping techniques (i.e. field mapping). Currently, laser scanners are extended on a boom into the base of a stope to collect the data needed for creating a model of the area. One downside of this method is that laser scanners lose point cloud resolution as the lasers measure distances further away from the scanner location (Azhari et al., 2017). As a result, the highest portions of tall stopes, as well as any occluded portions blocked by parts of the

stope's irregular shape, are not effectively mapped. GSM uses this laser scanner practice combined with the Q index mapping in the surrounding areas for estimating the rock mass characteristics of the stope.

A study conducted by the National Institute for Occupational Safety and Health (NIOSH) extending from 2011 to 2015 reported that the leading cause of occupational fatalities in underground mining is fall-of-ground (NIOSH, 2017). These fatalities account for approximately one-third of all underground mining related deaths over the five year span. Large failures in the stopes in underground mines can become major threats to underground mine personnel. To ensure that rockfall in the stopes does not cause harm to anyone (or equipment), the stoping areas at GSM are barricaded. Barricading the open stope does not rule out all chances of potential failures that pose as hazards to underground personnel though, as rockfall can create catastrophic failures and air blasts that can result in injury or fatality when there is a lack of understanding of a rock mass. By collecting data on the structural features of the rock mass via a remote sensing technique, rockfall in the stopes can be predicted using geotechnical analyses. If a UAV can be navigated through the stope for data collection, there is a possibility for a more complete understanding of the stope's rock structure. Understanding the rock mass and its respective stability and hazards will ultimately create a safer mine.

4. UAV Systems

Because this project aims to introduce a UAV-based digital photogrammetric system for underground mining environments, it is preferred that the system be physically compact. The focus of the project involved developing an efficient process for characterizing inaccessible rock masses underground using off-the-shelf products. Two readily available UAVs, the DJI Phantom 4 Pro (P4P) and the DJI Matrice 100 (M100), were used to conduct research to test whether or not a UAV-based photogrammetric system could be used to gather geotechnical data from underground mine sites. Each system was tested with numerous hardware customizations to find the most appropriate solution for accomplishing the project goals.

The M100 was the platform originally selected for conducting research; however, due to issues experienced with the M100 obstacle sensing system, the P4P was also explored and tested as a potential platform for research consummation. The UAV systems consist of the main UAV body, a flight controller, an obstacle detection system, a lighting system, a battery, and a camera. A remote controller was used with each system to communicate with its respective flight controller on-board the UAV, so that the UAV could be operated manually. In addition, an iPad (or mobile device) was connected to each remote controller, so that the live camera point-of-view could be viewed by the operator via the DJI GO app for the M100 or the DJI GO 4 app for the P4P. Additional equipment, such as a landing pad, PPE (personal protective equipment), and georeferencing tools were used for conducting this research as well.

4.1. DJI Phantom 4 Pro

The P4P platform is a small UAV quadcopter, measuring about 350 mm (14 in.) diagonally. It comes “ready-to-fly” out of the box, with a built-in flight controller, redundant IMUs (inertial measurement units) and compasses, dual-band satellite positioning, a stock

camera, and a five-directional obstacle sensing system. Each of these features is elaborated in Appendix A: UAV Systems.

A lighting system was added to the UAV to facilitate flying in an underground mine, where on-board lighting would be the only light source. Multiple configurations of two separate lighting systems (Lume Cubes and Firehouse Technology lights) were tested on the P4P. The lighting systems were mainly tested to assess whether or not the on-board obstacle sensors could effectively avoid obstacles with on-board lighting as the only source of illumination. Image quality was also taken into consideration. For more information about the lighting systems tested for on-board lighting refer to Appendix A: UAV Systems.

4.2. DJI Matrice 100

The M100 is a larger, much more customizable quadcopter platform as compared to the P4P. It measures about 650 mm (25.6 in.) diagonally (DJI - The World Leader, n.d.). Unlike the P4P, the M100 must be assembled out of the box; although soldering the UAV is not required, the main construction requires connecting and screwing parts together. The M100 comes with all of the necessary parts for assembly of the UAV including the body, arms, legs, flight controller with an IMU, battery, battery compartment, propellers, a GPS, a propulsion system, and a remote controller. Other smaller parts like the camera gimbal mount and an expansion bay also come with the M100, but are not necessary for the UAV to function. The carbon fiber arms and body are much more rugged than those of the P4P, which are plastic. Off-the-shelf customizations provided by DJI for the M100 include adding a second battery, the DJI Guidance system for obstacle detection and avoidance, and a thermal or RGB digital camera. In addition, the system is designed so that other non-DJI items can be mounted to the UAV as well. However, the M100 N1 flight controller is designed to only communicate with DJI products.

The DJI Zenmuse X3 digital camera, lights, and DJI Guidance system were added to the M100 to accomplish geotechnical data collection in an underground inaccessible site. Similar to the P4P, four different lighting systems were tested on the UAV to allow navigation in an underground mine, obstacle sensing, and capture of quality imagery. Detailed specifications on the features that come with and were added to the M100 are included in Appendix A: UAV Systems.

4.2.1. Camera

DJI has developed off-the-shelf cameras that attach to DJI UAVs and allow for real-time video to be transmitted in 720p to the user's mobile device when the device is connected to the remote controller. The real-time camera preview can be observed in the DJI GO app through a connected mobile device/tablet. As with the P4P, the connected device stores a reduced quality version of the imagery captured, and the full-sized imagery is stored on a micro-USB that connects to the aircraft. For stability, smoother shooting, and camera positioning, a three-axis gimbal (pitch, roll, and yaw) is attached to the camera allowing it 120° of total vertical tilt and 360° of lateral rotation. Modes locking the gimbal in a specific direction or in first-person view, allowing control by a second remote, or realigning the camera view with the aircraft's orientation can all be toggled on and off in the DJI GO app. The DJI Zenmuse X3 camera was chosen to conduct this research. The specifications for the camera can be found in Appendix A: UAV Systems.

4.2.2. DJI Guidance System

Manual flight is utilized for accessing underground areas (unless autonomy is implemented); thus, an obstacle sensing system is necessary for flying without crashing in inaccessible areas. The DJI Guidance is a group of stereovision cameras and ultrasonic range

finders arranged in each direction (except upward) on-board the M100, which enable the UAV to sense and avoid obstacles (DJI GUIDANCE User Manual, 2015). Figure 3 shows an example of the different parts of each sensor and the Guidance system installed on the M100.



Figure 3. (Top) An example of one of the five sensors that use LED indicators to confirm if the Guidance system is being used for detecting obstacles through the DJI Guidance cameras and ultrasonic sensors (DJI GUIDANCE User Manual, 2015) and **(Bottom)** the DJI Guidance mounted to the bottom of the M100 UAV.

A central processor called the Guidance Core is connected to each sensor so that it can collect and process data to send to the flight controller. The Guidance system comes with a mounting kit and all materials necessary for assembly. The Guidance may be mounted on the top or bottom of the UAV as long as the view of the stereo cameras is not obstructed. The downward facing sensor is not used for obstacle sensing, only for positioning (DJI GUIDANCE User Manual, 2015). In addition, the Guidance system has blind spots where obstacles cannot be detected, illustrated in Figure 4. The Guidance requires calibration for each new site. Details for Guidance system calibrations are in Appendix A: UAV Systems.

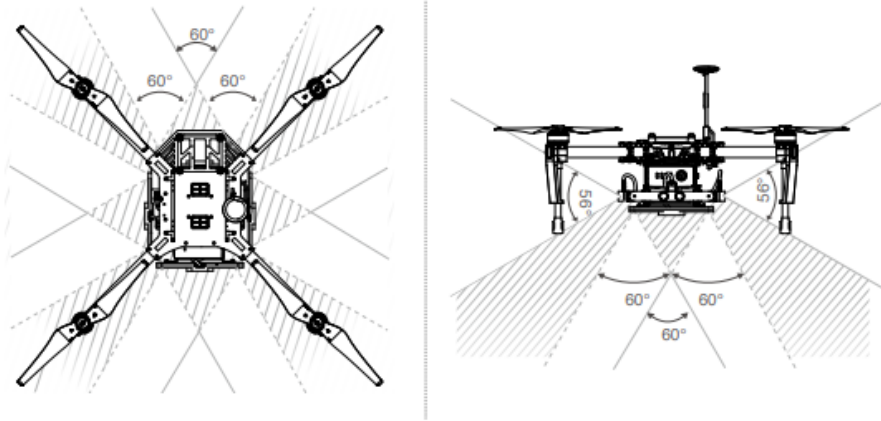


Figure 4. DJI Guidance sensor ranges and blind spots (DJI GUIDANCE User Manual, 2015).

If the operator is viewing the real-time camera imagery through a mobile device connected to the remote controller, a warning will appear on the screen when obstacles are being detected. An example of the obstacle detection warning is shown in Figure 5 in the middle of the screenshot. Within the DJI GO app, the user is able to select the obstacle avoidance distance at which the sensors were calibrated to avoid those obstacles. When the distance threshold is reached between the UAV and an obstacle (in the flight path direction), the UAV will halt movement in the direction of that obstacle until the obstacle is moved or the UAV is navigated away from that obstacle (DJI GUIDANCE User Manual, 2015). In the DJI GO app, specific maneuvers can be selected for the UAV's obstacle avoidance method. For example, the user can opt to set the UAV to maneuver around obstacles automatically, so when the UAV reaches the specified avoidance distance away from the obstacle it will find a route without obstacles in the flight path and then continue flight in the direction the UAV was originally attempting to fly.

The Guidance User Manual (2015) states that the Guidance system should not be flown in areas less than 3 m (10 ft.) wide or in crowded areas. In addition, other concerns in relation to the operation environment of the Guidance cameras and ultrasonic sensors are listed in the

Guidance User Manual (2015). Concerning the camera, flying over highly reflective, transparent, monochrome, moving, extremely dark (< 10 lux), or extremely bright ($> 10,000$ lux) surfaces is not recommended. Unclear textures and patterns or very repetitive patterns can cause issues with the Guidance system. Concerning the ultrasonic sensors, three different conditions are warned to possibly cause flight issues: 1) flying over surfaces that are inclined greater than 30° can cause sound waves to deflect away from the UAV, 2) flying over surfaces like thick carpet can absorb sound waves, and 3) flying over thin railing or fences may not allow for the sound wave to bounce off the surface back to the UAV. These specifications and warnings were all taken into consideration when testing the Guidance system in an underground mine environment.

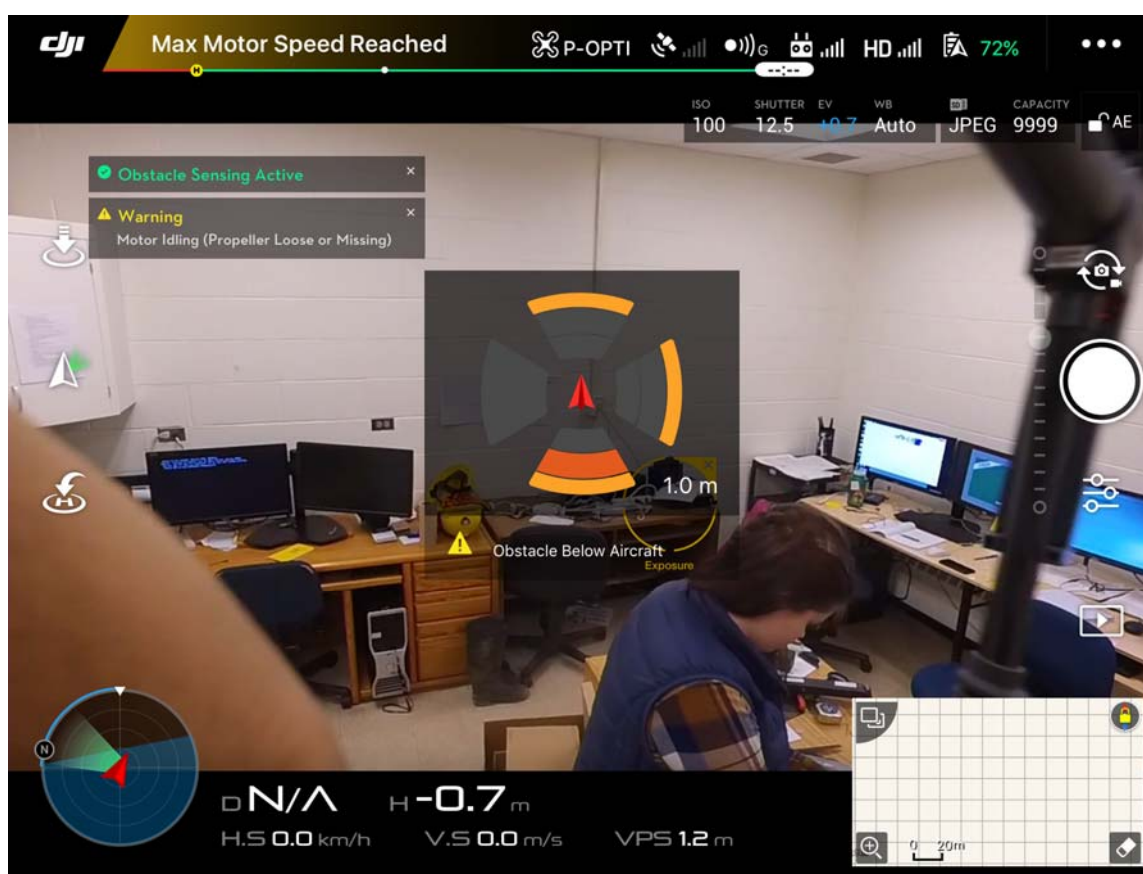


Figure 5. A screenshot of the warning that appears in the center of the connected mobile device screen when obstacles are being detected by the DJI Guidance system that is on-board the M100.

4.2.3. On-board Lighting Systems

Four on-board lighting systems were investigated to find the best system for capturing imagery and detecting obstacles in an underground mine environment. Like on the P4P, the Lume Cubes and Firehouse Technology lights were tested on the M100. The specifications for the Lume Cubes and Firehouse Technology lights are found in Appendix A: UAV Systems. In separate tests of each brand, four lights – one connected to each arm – were used for lighting the environment surrounding the UAV. The stock connectors for the lights were used to connect the two systems on the arms of the M100 and are shown in Figure 6. In some cases, extra rubber was used to more securely tighten the connectors around the arms of the aircraft.



Figure 6. *Left:* Lume Cube and connector used for attaching Lume Cubes to M100, *Right:* Firehouse Technology Light and connector used for attaching the Firehouse Lights to the M100.

Additionally, two Stratus LED systems were tested on the UAV: Stratus 100W LED Modules and Stratus ARM LED Modules. Each light in the two systems produce 13,000 lumens individually and require partial assembly, including soldering of parts. The Stratus 100W LED Modules weigh almost twice as much as the ARM LEDs, because of the larger heat sink and

connected fan. The ARM LEDs rely on the propellers for cooling and consequently use a much smaller heat sink. Both the 100W LED Module lighting system design and the ARM LEDs lighting system design consisted of two lights – one facing downward and one facing forward. To connect the 100W LED Modules to the UAV arms, the Firehouse Technology stock connectors were used as shown in Figure 7. More specifications on the Stratus LED lighting systems that were tested are located in Appendix A: UAV Systems.

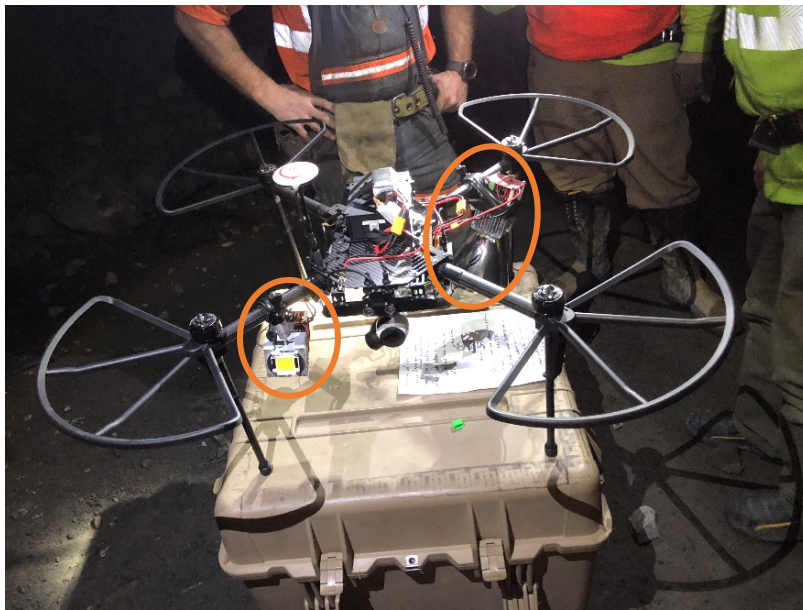


Figure 7. Photograph of the M100 underground photogrammetry set-up with the Stratus LED 100W LED Modules (circled) attached on adjacent arms.

5. UAV Flights: Preparation, Testing, and Data Collection

The first months of the project timeline were spent researching UAVs and off-the-shelf, UAV-compatible obstacle detection and avoidance systems, cameras, and lighting systems. After the DJI Matrice 100 UAV was purchased, along with the DJI Guidance system, it was assembled and calibrated. Prior to flying the UAV, all calibrations, tests (e.g. IMU test), and firmware updates must be applied to the UAV system. Initially, two lighting systems were purchased for testing on-board the UAV, but when they proved to be deficient, two additional lighting systems were purchased for testing on the M100 as well. A number of issues were encountered with the M100 Guidance and were difficult to troubleshoot and resolve due to lack of documentation and effective customer service from DJI. During the time that the M100 Guidance was not functional, the P4P was tested and considered as a potential replacement platform for capturing imagery of inaccessible areas in underground mines. Each UAV required different customizations for accomplishing the project goals.

Extensive practice flights with the UAVs were performed in GPS-denied indoor environments at many different locations. The UAVs were rarely flown outdoors due to the Montana weather conditions once the UAV was assembled, and the fact that GPS-signal is available (unlike in an underground mine). A couple lighting tests and practice flights were conducted underground at GSM and at the Underground Mine Education Center (UMEC) on Montana Tech's campus. Appendix A: UAV Systems, provides step-by-step methods taken when flying indoors, outdoors, and underground as well as for compass/IMU calibration. Some of the steps are specific to GSM protocols, and might not be necessary at other locations.

5.1. P4P and Associated Systems Testing

During the rearranging, recalibration, and retesting of the Guidance system for the M100, the P4P was considered as a potential platform for the UAV photogrammetry research. When considering using the P4P for a photogrammetry platform, multiple combined lighting and obstacle detection tests were performed in the basement of Montana Tech's Mining and Geology (MG) building. Three additional tests were performed as well: 1) to practice flight while only relying on the camera view on the mobile device, 2) for evaluating out of LOS communication between the UAV and remote controller, and 3) to practice flight in underground environments. The three tests were, respectively, conducted in the MG building, FEDEX garage, and UMEC.

After performing any necessary calibrations or firmware updates, the flight plans and goals of each test were discussed with the UAV group members who were helping with the experiment. Typically, tests began by setting the flight mode to P-mode, setting up lighting for the tests (external or on-board lighting), and checking the UAV and camera settings in the DJI GO 4 app. Most testing was conducted in P-mode, because A-mode caused significant drifting and did not use the on-board obstacle detection system. When flying in the FEDEX garage, the operators practiced navigating the UAV using only the real-time view available through the mobile device connected to the remote controller. The operator relied on obstacle sensing and avoidance (in P-mode) and the live-view feed for UAV operations. Just as in an underground mine, GPS-signal was not available during flight. Two spotters were present and alert during the flight to notify the operator if he or she was approaching an obstacle that was out of the LOS of the UAV camera. The spotters rarely had to warn the operator of obstacles, and no impacts or crashes occurred during these flights. This experiment also provided an opportunity for the operators to practice the elliptical flight pattern that was expected to be used for future stope flights.

For the out of LOS experiment, the UAV was flown around the corners of the MG basement hallway and partially up the stairwell, halfway to the first floor (Figure 8, left). All hallway and stairwell lights were used during the flight, because the focus of the flight was solely on whether or not the communication between the UAV and remote controller remained when flying out of LOS. Spotters were used to ensure pedestrians did not enter the area during flights. The UAV was flown about 20 m (65 ft.) down the hallway and around two corners, but was crashed in an attempt to turn the UAV around to return to the starting location. The crash was not due to loss of connection between the UAV and the remote controller, rather it was due to the inability to avoid obstacles in all directions when flying in a confined space in P-mode.

Later, a state within P-mode called Tripod Mode was tested in the UMEC (Figure 8, right) and found to be the preferable option for conducting underground flights. When flying in areas where terrestrial lighting was available, the UAV obstacle sensing system successfully detected and avoided obstacles, preventing the UAV from crashing. Tripod Mode restricts flying at high speeds, but underground flight for photogrammetry did not require high speed flight. The main advantage of Tripod Mode is that the side infrared sensors are active during flight, unlike in normal P-mode. Using this setting for the out of LOS flight in the MG building could have helped to avoid crashing, since the left side of the UAV was the side that crashed into the wall. Obstacle sensing on all sides of the UAV made navigating the UAV in a confined space much easier.

Lighting and obstacle avoidance tests were normally conducted at night and with all hallway lights turned off in the MG basement. After many trials using on-board lighting with the P4P, it was determined that the P4P could not stably carry the required load for obstacle sensing to detect obstacles located over 3 m (10 ft.) away from the UAV. The lighting must be able to

light a rock wall from several meters away; otherwise, the system drifts due to inability to detect its surroundings. When utilizing the higher lux lighting system, the P4P would tend to fly unstably due to the excessive payload. The P4P was eliminated as an option for underground photogrammetry in large inaccessible areas because terrestrial lighting cannot be utilized in such scenarios and available lighting systems that provide adequate illumination are too heavy for the UAV to carry.



Figure 8. Photos of (*Left*) an out of LOS flight with P4P in the basement of the MG building and (*Right*) the P4P flight in UMEC where Tripod Mode was tested and terrestrial lighting was used to light the rock face.

5.2. M100 and Associated Systems Testing

The M100 was tested over the course of five months, focusing mainly on lighting and the Guidance system. Only a few outdoor flights were performed using the M100, because of the initial issues with obstacle detection and the winter weather in Montana. The DJI Matrice 100

specifications state that the UAV should only be operated in temperature ranges of -10°C to 40°C (14°F to 104°F) (DJI Matrice 100 User Manual, 2017). The winter months in Montana, when testing was occurring, were often colder than -10°C (14°F). In addition, the UAV battery life is significantly reduced when used at low temperatures. From the first outdoor flight experience, it was learned that the compass should be positioned so that it faces the nose of the aircraft and the UAV should always be flown with the camera attached. Most other outdoor flights were conducted low to the ground while testing the Guidance.

Practice flights for testing the Guidance system indoors were conducted at various locations including in the Health Physical Education Recreation (HPER) Complex and the high bay in the Engineering Lab/Classroom (ELC) building on Montana Tech's campus, a horse arena, and the Butte Ice Center. Lighting tests were conducted underground at GSM to compare the four lighting system options: Lume Cubes, Firehouse Technology lights, Stratus LED 100W Modules, and Stratus LED ARM Modules. Additionally, an experiment testing the M100's ability to communicate with the remote controller around the corner of an intersection drift (out of LOS) underground at GSM was executed. All testing began by performing calibrations or firmware updates when necessary, marking off the area in which the UAV would be flown, preparing the UAV set-up for the specific test, setting the flight mode (usually to P-mode), checking the UAV and camera settings, and discussing the flight plans and goals with the UAV group members present.

5.2.1. DJI Guidance System Testing

The DJI Guidance is designed to provide obstacle detection and avoidance, which is an important feature for flying the M100 out of LOS without crashing. Prior to testing the Guidance system on the M100, the cameras on the Guidance system were calibrated for detecting obstacles

at a specified distance. Preparation and testing of the Guidance system was accomplished using the procedure outlined in Appendix B: Flight Procedures in association with the DJI Assistant app.

Over about a four month timespan, the obstacle detection system on-board the M100 (the DJI Guidance) failed to detect obstacles. Repeated troubleshooting and rearranging of the system only ended in crashes and/or failed obstacle detection. Most testing was performed with the obstacle detection system mounted on top of the aircraft to avoid interfering with the UAV camera. The DJI Phantom 4 webpage (Phantom 4 Pro - Professional aerial filmmaking made easy, n.d.) recently released information about obstacle detection issues with traditional ultrasonic sensors due to the vibration of the propellers. The same issue is likely applicable to the DJI Guidance ultrasonic rangefinders too, explaining the repeated obstacle detection failures. This fact was discovered after multiple tests with the Guidance system mounted on top of the UAV – where they are most susceptible to propeller vibrations.

After the system was installed underneath the body of the UAV for a second time to avoid propeller interference and behind the camera gimbal, it operated successfully. Initially, the front sensor obstructed the clearance of the UAV camera gimbal, so the front sensor was mounted on top of the UAV facing upward when the rest of the system was mounted below the UAV. The placement was only used as a temporary location, and the sensor was still calibrated as if it were positioned facing the front of the aircraft. Tests performed with this configuration revealed that the obstacle sensing warnings that show on the screen of the controller, as seen in Figure 5, only appear when the calibrated UAV battery is used in the M100. The calibrated UAV battery refers to the specific battery with which the calibration of the Guidance system was performed. Use of a non-calibrated battery still allows for obstacle sensing and avoidance, but

obstacle warnings are not displayed on top of the real-time feed shown on the connected mobile device/tablet. With this knowledge, consistent successful obstacle avoidance was achieved. The front sensor was then rearranged so that it faced forward under the propellers while attached to the main body of the UAV in front of the camera gimbal. After recalibration, the system was tested and it was determined that it was able to successfully detect and avoid obstacles in all directions (except those located above the system). This configuration was identified to allow for confident use of the Guidance. These discoveries are significant since there is little troubleshooting support and documentation available for the DJI Guidance system.

5.2.2. On-board Lighting Systems Testing

Two approaches were taken to test the four lighting systems on the M100. The first approach used video footage taken using the UAV camera to determine the settings and lighting that is preferable for capturing imagery in an underground mine. Controlled tests were conducted varying imagery settings and the lighting system used. The second approach used a light meter for determining lux outputs of the four lighting systems. It aimed to determine the ranges at which the on-board lights would allow for the Guidance system to detect obstacles based upon the DJI specifications for the amount of lux required for operation.

The underground controlled lighting tests at GSM were organized for determining the preferable camera settings for underground video imagery. Two Stratus 100W LED Modules (very similar to Stratus ARM LEDs) and a pair Lume Cubes were used, separately, for the controlled testing. One 100W LED Module was attached facing toward the front of the UAV, while the second light with a parabolic reflector was attached facing downward during the tests. In the Lume Cube tests, both lights were aimed forward. Due to time limitations for testing at GSM, only these two lighting systems were used to test the lighting using the video settings

approach aforementioned. The lighting systems chosen for testing were narrowed down through expected outcomes, derived from the previous P4P Guidance tests in the dark hallways of the MG building. The P4P obstacle detection system could detect obstacles at a maximum of 3 m (10 ft.) away from the object, with two Lume Cubes facing in the direction of the obstacle; when the same scenario was enacted, but with two Firehouse Technology lights, the maximum distance at which an obstacle was detected was at 2 m (6 ft.) away from the obstacle. Based on the results of these tests, the Lume Cubes were prioritized as a potential underground lighting system over the Firehouse Technology lights. The 100W LED Module, known to be much brighter than the previously mentioned systems, served as a representative of the ARM LED, since the LED specifications between the two have few differences.

The other test parameters that were changed include the video formats (D-log versus Normal), frame rate and resolution (4K at 24 fps and 1080 at 60 fps), the two different lighting systems, and the use of diffuser paper on the LED Modules. Diffuser paper (LEE Filter: 410, Opal Frost) was used only on the 100W Modules, because it was predicted that the high number of lumens (13,000) might be too harsh for lighting the scene and the diffuser paper would serve as a way to reduce the harshness of the light by dispersing its rays. Table I shows all of the testing combinations.

The first apparent observation was that the diffuser paper did not improve imagery quality. Unwanted, excessive traces of light called lens flares appeared in the imagery captured using the diffuser paper with the lights. The lens flares created “light spots” on the imagery, blocking parts of the scene being captured. The issue of lens flares appearing in the imagery was eliminated when the diffuser paper was removed from the 100W Modules; thus, it was quickly decided that diffuser paper was not improving the underground imagery.

Table I. Lighting control test combinations used underground at GSM and corresponding image quality.

Stratus LEDs	4K	Normal	diffuser paper	24 fps	Poor quality
	4K	Normal	no diffuser paper	24 fps	Good quality
	4K	D-log	diffuser paper	24 fps	Poor quality
	4K	D-log	no diffuser paper	24 fps	Good quality
	1080	Normal	diffuser paper	60 fps	Poor quality
	1080	Normal	no diffuser paper	60 fps	Good quality
	1080	D-log	diffuser paper	60 fps	Poor quality
	1080	D-log	no diffuser paper	60 fps	Good quality
Lume Cubes	4K	Normal	n/a	60 fps	Moderate quality
	4K	D-log	n/a	60 fps	Too dark
	1080	Normal	n/a	60 fps	Moderate quality
	1080	D-log	n/a	60 fps	Too dark

When comparing the Lume Cubes versus the 100W LED Modules, the Lume Cubes did not light the drift nearly as well as the 100W LED Modules. The imagery captured using the 100W LED Modules was much clearer than that captured with the Lume Cubes. Additionally, after the first two tests with the Lume Cubes, the lights dimmed significantly due to the reduced battery charge. The dimming of the Lume Cubes in such a short time (about five minutes) caused them to be eliminated as a potential lighting source for underground UAV-based imagery.

For the second light test approach, light measurements were taken using a Dr. Meter LX1330B light meter to determine the true lux that each lighting system was projecting onto an underground rock face at varying distances (Turner et al., 2018). Because the Stratus LED lighting systems are very similar with respect to light output, only one 100W LED Module was tested, once with the parabolic reflector and once without it. Although the Firehouse Technology lights and the Lume Cubes had been ruled out of potentially being used for on-board lighting, they were still included in the tests, which were conducted in a drift at GSM. Lux measurements were recorded at 3, 7.5, 15, and 30 m (10, 25, 50, and 100 ft.) away from the rock face. In total,

16 measurements of lux were recorded, four measurements for each of the four lighting configurations: a pair of Lume Cubes, a pair of Firehouse Technology lights, a Stratus LED with a parabolic reflector, and a Stratus LED without a parabolic reflector.

The results (Table II and Figure 9) from the lux measurements taken at varying distances with each lighting system confirm that the Lume Cubes and Firehouse Technology lights are not appropriate for accomplishing the project goals or for the Guidance system to detect obstacles at short distances (Turner et al., 2018). The Stratus LEDs provide sufficient light for the Guidance system to function properly and still maintain quality image capture. The ARM LED Modules were determined to be the best choice for underground data collection because they were not as heavy as the 100W LED Modules and the UAV was limited by payload capacity.

Table II. Measured lux values from a controlled test of the four lighting systems considered for use on the M100 (Turner et al., 2018).

Distance at which lux was measured [m (ft.)]	Lighting System (number of lights) and Measured Lux			
	Lume Cubes (2)	Firehouse Tech. (2)	Stratus LEDs w/ reflector (1)	Stratus LEDs w/o reflector (1)
3 m (10 ft.)	105	16	4500	550
7.5 m (25 ft.)	18	3	1250	75
15 m (50 ft.)	4	0.1	300	17
30 m (100 ft.)	1	0.1	75	4

A number of video formats are available on the Zenmuse X3, but most are used for specialty cases that are not in the scope of this project. Other than the Normal setting, the D-log video setting was tested because it allows for a wider range of light editing when areas are over- and/or under-exposed. For an underground scenario where the lighting for imaging is not constant, the D-log setting seemed to be an appropriate solution to varying exposure throughout video stills. Typically, D-log imagery appears to look greyer than it appears to the human eye; however, this greyness may be adjusted for during post processing. For this site, little difference

between the D-log imagery and the Normal imagery was observed, likely because the rock being captured is grey to tan in color. Furthermore, the normal imagery did not appear to have significant issues with over- or underexposure. Consequently, it was decided that Normal imagery was sufficient for creating 3D models for mapping, since the learning curve for editing D-log imagery did not comply with the short project timeline.

It was difficult to compare the higher resolution of the 4K video to that of the 1080 because a 4K resolution monitor is required for viewing the 4K data at its true resolution; hence the deciding factor between the two resolutions was their frame rate capability. Because the Zenmuse X3 only allows for up to 24 frames to be captured per second capturing video in 4K, capturing clear frames of flight imagery in a dark underground mine was problematic. When reviewing the imagery from both 4K and 1080 shots, the 60 fps used for capturing the 1080 resolution imagery provided clearer and more reliable video still frames (due to the higher frame rate) that could be used for creating a 3D model. The 1080 resolution imagery also produced significantly smaller file sizes making the data more workable.

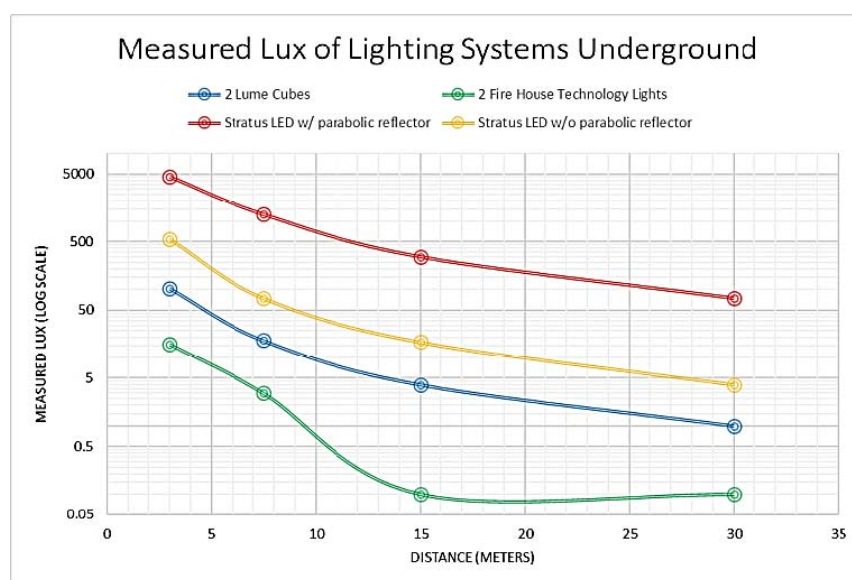


Figure 9. Measured lux as a function of distance away from a rock face for the four different lighting systems for use on the M100 tested underground at GSM (Turner et al., 2018).

5.2.3. UAV/Remote Controller Communication Testing

On February 19, 2018, the M100 was flown out of LOS in a drift at GSM to determine if the remote controller and M100 flight controller would maintain communication. Furthermore, the flight was performed to delineate the range of safe operations for collecting structural data on a UAV-based platform in the underground environment. The pilot stood just behind the corner of the intersection of the 895-102 drift and flew the UAV around the corner and down the drift. Once the UAV was around the corner, and out of LOS, the pilot relied on the live-view camera feed for maneuvering the UAV along the drift. The UAV reached up to about 38 m (125 ft.) out of the pilot's LOS during the test. To clarify, the measurement of 38 m is the total distance to the end of the drift in which the UAV was flown and not necessarily the maximum distance that could have been reached before the remote controller lost signal to the UAV. When flying out of LOS around the corner of the 895-102 intersection of connecting drifts, no communication errors were experienced between the UAV and the remote controller (including the live-feed imagery). The maximum distance at which the UAV remained in connection with the remote controller was not determined.

5.3. Georeferencing Technique Testing

The georeferencing technique was tested in the 895-102 drift on February 19, 2018, as well. The georeferencing system consisted of using a Trimble total station, reflectors, a car battery (to power the total station), a survey tripod, a flashlight, and a paintball gun with paintballs and a compressed air canister. The paintballs were shot into the inaccessible area, and those points were measured using the total station. To achieve the goal of georeferencing a photogrammetric point cloud captured in an inaccessible area, two main questions needed to be resolved:

1. Can the paintball marks be located and measured successfully with a total station?
2. Can the paintball marks be located within the UAV-based video imagery?

To begin testing the paintball georeferencing method for marking control points in areas that cannot be accessed in the mine, the total station was positioned and leveled in an area within LOS of the existing control points along the ribs of the mine and within LOS of at least a portion of the area where imagery data collection would take place. Reflectors were placed along the ribs where known survey points exist, so that they could be measured using the total station (Figure 10). A flashlight was used to illuminate the reflector from a distance. Then a resection was performed using GSM's Trimble total station and the two previously existing points with known coordinates that were located along the ribs of the mine drift. A resection uses two (or more) known points to find the coordinates of a third. In this case, the third point is the location of the total station. If the location of the total station is known, then the total station can determine the coordinates of the paintball marks, which were used as control points. This allows for control in the model without the need for GPS-signal.



Figure 10. Reflector installed on the mine rib at a known coordinate (on the local mine grid) that is used for determining the total station location by performing a resection.

To create marks for control points, paintballs were shot along the ribs of the 895-102 intersection of GSM in locations that could be measured with the total station (within the LOS of the total station) as seen in Figure 11. Three consecutive shots were aimed at a single point in order to create a pigmented color mark on the rock. Bright yellow paintballs were used so that they could be easily identified against the rock surface. After marking the area with paintballs at varying heights, the total station was used to measure the coordinates of each of the paintball control points. To help make the process more efficient, one UAV team member used a powerful flashlight to illuminate the paintball marks, while another team member measured the marks using the total station. It is important to note that three control points is the minimum number of control points necessary for building a georeferenced 3D model. It is not guaranteed that all points will be visible in the imagery, so it is good practice to capture and record more than three points. The paintball points were successfully measured, and it was later confirmed that the paintball marks could, indeed, be located within the video imagery captured of the 895-102 drift. This method also proved successful when measuring paintball control points in the NEV Stope.



Figure 11. (Left) UAV team member shooting paintballs onto ribs for creating control points and, (Right) Control points created on the ribs in yellow (blue arrows are pointing to paintball marks). For scale the height of the paintball gun operator in the image to the left is 1.7 m (5ft. 7in.) tall. In the photo to the right, the wire mesh has 25 mm (4 in.) spacing and the UAV (with the propeller guards) measures about 1.2 m (4 ft.) diagonally.

6. Underground Data Collection

To prepare for a stope flight and to verify that underground UAV photogrammetry can be used for creating models from which geotechnical structures can be derived, a drift flight was conducted in the 815-102 drift on March 1, 2018. Because the georeferencing technique had already proven to work underground, the focus of this test was only to ensure that underground video imagery could be used to produce a model that could in turn be used for mapping. After successful data capture in the 815-102 drift, the NEV Stope at GSM was flown on March 2, 2018, while video imagery was collected. In this case, the georeferencing technique was utilized, so that the structures identified in the 3D model could be mapped in their true orientation. All video was captured in 1080 resolution at 60 fps in the Normal imagery setting (not D-log). The high frame rate was chosen to ensure clear imagery with significant overlap between the video stills.

6.1. Flight in the 815-102 Drift

The main goal of this flight was to capture overlapping imagery in an environment similar to the planned stope flight. A drift was selected because the UAV could be recovered if it crashed. The UAV was not flown out of LOS in this particular drift. A front-facing and downward-facing Stratus ARM LED Module were mounted on the UAV to provide light for the camera and Guidance system. The downward light had a parabolic reflector attached to it to increase the lux of the light beam. Increasing the lux allows the downward sensor on the UAV to sense the ground surface at greater heights than without the reflector attached. As long as the ground can be detected, the aircraft is able to maintain altitude. The UAV was flown down the drift and back toward the starting position while facing the same rib. A ventilation bag was hanging from the back of the drift, so there was only about 3.5 m (12 ft.) between the sill

(ground) and the ventilation bag where the UAV could fly. The width of the drift was about 4.5 m (15ft.).

The rock face was adequately illuminated by the lighting on-board the UAV and the underground UAV video was captured successfully in the 815-102 drift without crashing; however, there was one incident in which the behavior of the UAV did not correspond with the remote controller commands being given. The UAV was drawing closer toward the rib, and for approximately 15 seconds it would not respond to attempts to direct it away from the rib. The problem was not diagnosed, and was dismissed once the UAV responded to the remote controller again. The UAV was being flown in P-mode, so this behavior should not have been permitted because the distance between the UAV and rib was about 1 meter (3.3 ft.) versus the 2 m (6.6 ft.) calibrated obstacle avoidance distance. Additionally, issues flying over puddles of water were also observed during this flight; the UAV tended to have difficulty maintaining altitude when flying over the water, most likely due to the highly reflective surface of the water.

The overlapping video still imagery was used to build a model of the 815-102 drift to confirm that underground UAV imagery can be used to create an adequate model for mapping structural data – one of the primary goals of the project. Achieving the goals of the project will contribute to the ability to successfully fly and collect data in drifts allowing also for a) inspections of a recently blasted drift where the ground is unsupported, b) progressive models to be made with each new blasted portion of the advancing drift, serving as a record of the blasts, and c) a 3D representation and record of the geological and geotechnical features of each blasted face.

6.2. Flight in the NEV Stope

After successfully flying in the 815-102 drift on March 1, 2018, the UAV was flown in the NEV Stope at GSM. The stope is about 6 m (20 ft.) wide, 46 m (150 ft.) tall, and 122 m (400 ft.) long. Figure 12 is a model of the NEV Stope provided by GSM employee Brian Dale, showing the three drawpoint locations (DP1, DP2, DP3) with respect to the stope and drift access to the stope. Drawpoint 1 was chosen for the entry point for the flight into the stope because it had the most steeply inclined muck pile (the pile of loose ore-laden rock that collects at the bottom of the stope after blasting). By choosing the drawpoint with the steepest muck pile, there was a better chance of recovering the UAV if it crashed.

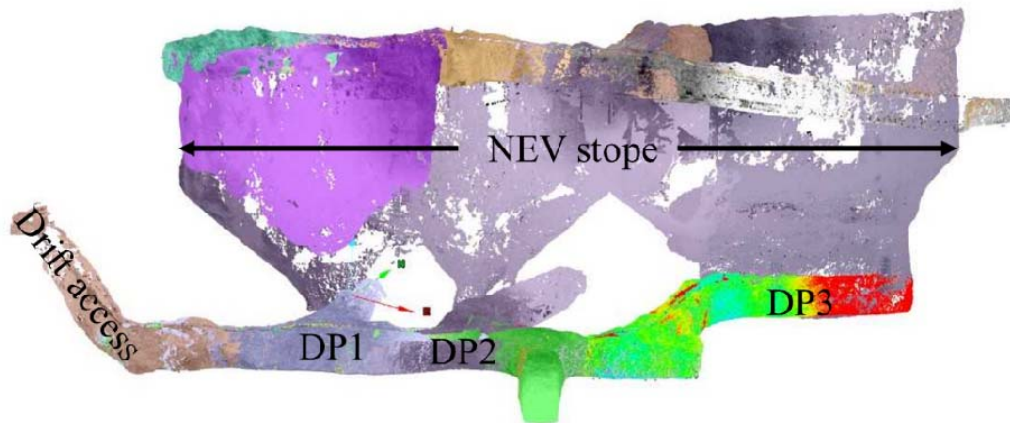


Figure 12. GSM's ISite point cloud of the NEV Stope (modified, Brian Dale). For scale, the height of the drawpoints (in the vertical direction) is approximately 5 m (16 ft.).

Before the flight, the paintball georeferencing technique was carried out using two known mine survey points in the drift access as the control points for the resection. The coordinates of four paintball marks within the stope were recorded, producing four ground control points in drawpoint 1, listed in Table III. Only three of the four ground control points were easily identified in multiple images from the stope flight; as a result, only ground control points 1, 2,

and 4 were used for georeferencing the model. For an area of the size captured, additional control points would have been ideal for creating a more accurate model.

Table III. Ground control points (GCPs) that were measured in drawpoint 1 of the NEV stope using the Trimble Total Station and two known survey points. These values are in the local mine coordinate system.

GCP ID	Easting (ft)	Northing (ft)	Elevation (ft)
GCP1	22966.853	26061.000	4346.021
GCP2	22955.983	26046.395	4344.019
GCP3	22968.403	26022.349	4328.174
GCP4	22967.294	26016.298	4319.216

A very short test flight was successfully conducted in the access drift to the NEV Stope to ensure that the M100 was operating properly before launching it into the stope. The intended flight path was to first cover the lower portion of the stope near drawpoint 1 in an elliptical motion, and then to move upward to capture overlapping data following the same pattern. All underground flight methods were followed to conduct this flight (Appendix B: Flight Procedures). Once drawpoint 1 was captured, the intent was to capture the other two portions of the stope near the drawpoint entrances, changing the UAV battery in between, if necessary.

The initial portion of this spiral flight path went smoothly, but once the UAV was out of LOS, it proved difficult to keep track of the UAV location with respect to the starting position. Significant amounts of water dripping from above, along with a large amount of dust in one portion of the stope, caused additional issues with keeping track of the UAV's position. At one point, the UAV propellers stirred up enough dust to cause the pilot to lose track of the location and position of the aircraft. After 30 seconds in the dusty area, the UAV was located by using the downward facing light as a visual reference, and the pilot continued to operate the UAV, occasionally moving the camera to capture more imagery while hovering. The obstacle detection system was operational for the whole flight, but in the last few seconds the UAV was drawn into the rock face (similar to the previous observation when flying in the 815-102 drift) and crashed.

The Guidance appeared to be functioning during this time since it showed that the aircraft's distance from the rock face was decreasing; however, the pilot attempted to direct the UAV away from the wall, but the UAV was unresponsive and crashed. When the UAV crashed, it was located out of LOS and was facing in the opposite direction of the take-off position (facing the pilot). Fortunately, the UAV system rolled down the muck pile and was recovered safely. Suitable imagery was captured to build an incomplete model of drawpoint 1 of the NEV Stope at GSM, providing more geotechnical data than were available without the model.

7. Mapping and Modeling Software and Results

Two photogrammetry software sets were selected for inclusion in this study for comparing modeling and mapping processes and outputs. Tonon and Kottenstette (2006) reported on a workshop where ADAM Technology proved to be a leading software for digital photogrammetry. ADAM Technology's 3DM Analyst, 3DM CalibCam, and DTM Generator are commonly used throughout the mining industry, as well as at Montana Tech, for geologic modeling and mapping. After evaluating a number of other photogrammetry software packages (Becker et al., 2018), Bentley ContextCapture was selected based on its ability to produce the most complete 3D models of the underground environment using UAV video imagery. Because ContextCapture does not have a function for mapping geologic structure, Split Engineering's Split-FX was selected to use in conjunction with ContextCapture.

Both of the software packages have specific requirements for creating 3D models, as well as their own advantages and limitations. In the software packages used for model building, there is the option to run the model as a "controlled" model, defined by georeferenced control points that are oriented and scaled correctly relative to the earth or a local coordinate system, or as a "relative" model, defined by matching points that the software finds between images. Georeferenced controlled models are also referred to as "absolute" models. In terms of photogrammetry, georeferencing refers to assigning coordinates to points in images that have been surveyed on a specified coordinate system (Birch, 2006). By assigning the actual positions of the points on a coordinate system, the imagery is scaled to the actual life-size coordinates and oriented correctly in space. A relative model is able to maintain dimensional accuracy and orientation, but on an arbitrary scale. With a correctly-oriented life-size scaled model, measurements taken on the 3D model will represent the actual measurement as if it were taken in

the field. For this project, the models of the 815-102 drift were constructed as relative models, while the NEV Stope models were constructed with a georeferenced orientation on the local mine coordinate system.

Typically, surveyed control point markers or spray painted points are used for defining locations in which coordinates will be measured when creating absolute underground 3D models of mines. For photogrammetry projects, it is good practice to spread the control points across different areas of the model. When control points are distributed throughout the model, distortion is reduced, providing a truer representation of the area being modeled. However, spreading control points across an area that cannot be accessed is challenging and may not be possible. In this project, a paintball gun was used to make paint marks on the rock faces that were within the area to be modeled and also within LOS of the surveying equipment.

7.1. ADAM Technology Software Approach

In ADAM Technology's software package, 3DM CalibCam has the function to build 3D point clouds, meshes, and surfaces. The general workflow includes calibration, an exterior orientation, and bundle adjustment (Lingen, 2011). Once the lens and camera combination are defined (and calibrated), a photo project can be started in 3DM CalibCam for the point cloud construction. Then to create a surface model from the imagery, digital terrain models (DTMs) must be generated. DTMs are generated for portions of the model that are divided by the software, and then can be merged into one DTM. The individual DTMs and the merged DTM are all created using the DTM Generator in ADAM Technology.

After generating DTMs, the merged DTM or multiple smaller DTMs can be loaded into 3DM Analyst for mapping the geologic structure of the rock mass. A feature definition file (FDF) has to be created to map different features in the 3D-view. All features were mapped

manually for both underground data sets. Once the structural features are mapped, the stereonet can be viewed, and average orientations can be calculated for specific joint sets mapped on the model. Within the stereonet window, 3DM Analyst allows for manipulation of the data set, like assigning a joint set color to a grouping of points on the stereonet. More information about the workflow and requirements of ADAM Technology are attached in Appendix C: Workflow and Procedures.

7.2. ContextCapture and Split-FX Software Approach

The other photogrammetry software used was Bentley ContextCapture, a newer software package that was developed to be optimized for UAV-based photogrammetry, which typically produces many images (Bentley, 2018). The software uses a relative aerotriangulation to determine the relationships between the images and then constructs a production of the imagery (i.e. a 3D model). All images that were used in the model were used for the aerotriangulation. Other specifications on ContextCapture can be found Appendix C: Workflow and Procedures.

Split Engineering's Split-FX was used for mapping the modeled imagery constructed in ContextCapture. Because ContextCapture cannot export the point cloud data into a form that can be used directly by Split-FX, the ContextCapture point cloud in the laser (.las) file format was imported into a separate software (Agisoft Photoscan), so that the point cloud could be exported as a text (.txt) file. Then, the text file was imported into Split-FX specifying the ASCII (*.*) file type. The x, y, and z coordinates and the RGB values for the point cloud were defined upon import by assigning them to a data column (as prompted by the software). Once the point cloud was loaded, structures were identified and manually mapped on each of the underground models, separately. Sometimes a viewing orientation was stored during mapping in Split-FX to return to a specific view of the model repeated times. Like in 3DM Analyst, the structural data can be

displayed on a stereonet for analyses. The Bentley ContextCapture model that was built of the NEV Stope was also mapped using 3DM Analyst, by exporting an object (.obj) file from ContextCapture and loading it directly into 3DM Analyst. The point cloud, mesh, solid surface, and visible color solid surface of the stope were all viewable using the 3DM Analyst software.

7.3. Modeling and Mapping the 815-102 Drift as a Proof-of-Concept

The 815-102 drift mapping and modeling was used as a proof of concept confirming that UAV-based imagery collected in an underground mine drift at GSM could be used for constructing a 3D model on which structural orientations can be mapped. Stills from the video imagery were extracted for use in both photogrammetry software packages, about one second apart, totaling 170 photos. In ADAM Technology, the merged DTM was created with a relative orientation and resulted in a curved model shape (Figure 13). Without using defined ground control points, the model was unable to accurately represent the (straight) drift as it is found underground. In addition, a portion of the drift was not built by the software, creating a “hole” in the model. Structural features are apparent in the model and were easily mapped using 3DM Analyst (Figure 14). The stereonet for this model is not an accurate representation of fractures in the drift due to the fact that the model was not created with an absolute orientation, so it was not used for comparison against the mapped features in Split-FX. Also, the curvature of the model causes erroneous variation in orientation of joints that are closely aligned in real space. These mapped models successfully proved that UAV-based imagery captured underground can be used for modeling and mapping a rock mass.



Figure 13. A merged DTM (*top*) of one rib of the 815-102 drift at GSM created using ADAM Technology software with the plan view (*bottom*) of the drift to display the erroneously curved shape that the software produced. This model was constructed from UAV-based video stills.

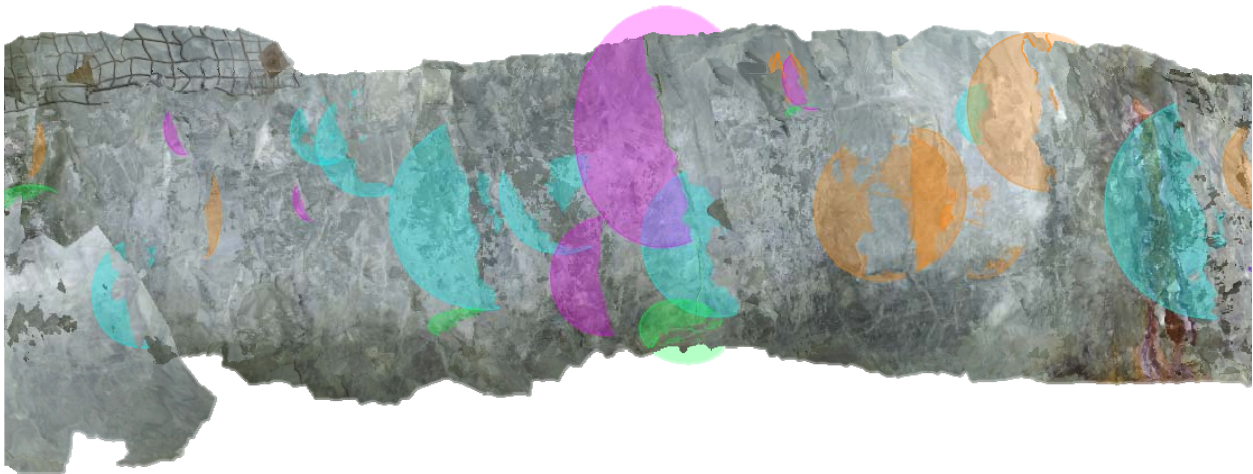


Figure 14. The 815-102 drift rib mapped (and modeled) using ADAM Technology software with color coded structure orientation; some joints demonstrate erroneous orientations of structures that are in the same set in reality.

A comparable 3D model was built of the 815-102 drift using Bentley's ContextCapture (Figure 15). The model created with ContextCapture was judged to be more successful in capturing the actual shape of the 815-102 drift, because the model produced is clear and represents the straight shape of the drift without gaps. Mapping features in Split Engineering's Split-FX was much more difficult than in 3DM Analyst. Mapping was performed on a very dense 3D point cloud in Split-FX, versus a 3D surface as in 3DM Analyst (Figure 16). Split-FX

does not allow for surface file format imports, but can create a surface from the imported point cloud. The meshed surface created using the point cloud in Split-FX was poorly constructed and introduced significant error to the model; hence, the point cloud was used for mapping instead.



Figure 15. Bentley ContextCapture model built of the 815-102 drift rib at GSM. This model was constructed from the same UAV-based video stills as the model constructed in the ADAM Technology software.

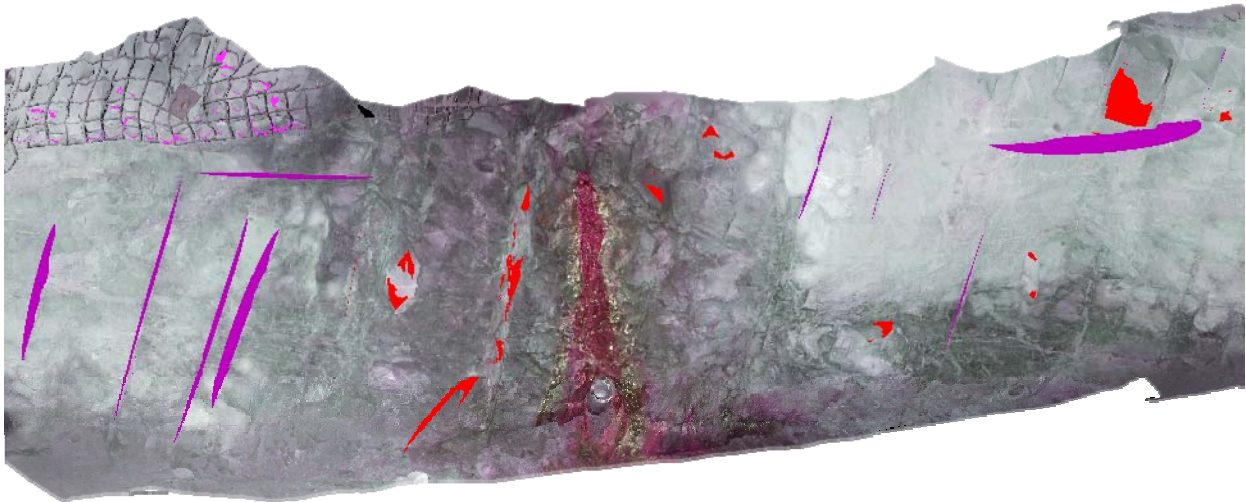


Figure 16. Structures shown in purple and red that were identified and mapped using Split-FX on the ContextCapture model of the 815-102 drift rib at GSM.

While working with Split-FX, several issues were encountered: the response to mouse movements was delayed and the response to the mouse dragging directions was not always logical. When mapping structures in 3D models, it is necessary to rotate and tilt the model to be able to identify and accurately measure 3D surfaces or fractures. Because the software was slow to respond to movements, the relation between different orientations of the rock surface was hard

to visualize, making structural measurements more difficult to acquire. Specific model orientations were stored within the project to replicate views in which multiple joints were to be mapped; this is necessary, since Split-FX resets the view of the model to the imported position (which was relative in this case) after mapping each structure on the model. Again, the stereonet was not used for this portion of the project since the model is a relative model.

7.4. Results from the NEV Stope

The NEV Stope was modeled and mapped using both software packages, with attempts to create absolute rather than relative models. Frames from the usable portion of the four minute stope flight were selected, one every second, and modeled in both 3DM CalibCam and ContextCapture. The total number of still frames used in each of the initial models was 225 images. Each model used three of the four ground control points surveyed with the Trimble total station. The attempted modeling using 3DM CalibCam was unsuccessful, but the ContextCapture model was built successfully. The model is considered to be incomplete, though, since it has holes where either bad data exist or no data exist (Figure 17, top); thus, another model was constructed in an attempt to fill the holes. For the second model, a still image sampling rate of every 0.5 seconds of the usable portion of the video produced 450 extracted frames. Only 446 frames were used because four of the images captured the high concentrations of dust floating around the camera rather than the surrounding rock face. Figure 17 (bottom) shows that the model of the stope built with approximately double the number of images as the first model created a slightly more complete model, with subtle differences. The general shape of the portion of the stope corresponding to the first drawpoint entrance can be clearly seen in each model. Large holes are present in both models due to the flight path execution. Figure 18 shows the 446 image model in two different zoomed views. The directions in which the camera was

facing during video capture can be seen. From the figure, it is evident that the camera did not capture imagery in the areas where the holes exist because it was not pointed toward the rock face. Another factor that contributed to the holes is the lack of quality imagery in these specific locations. During a portion of the flight, a highly dusty area was encountered, and the imagery in that area had to be discarded since the light was reflected by the particulate matter in the air. In addition, little ambient light was available when the camera on the UAV was not facing the forward direction and when the UAV did not approach the rock surface closely enough for sufficient illumination.

Structures were mapped on the point cloud model using Split-FX and on the visible color surface in 3DM Analyst. Figure 19 shows some of the features mapped in Split-FX. When mapping structures in Split-FX, glitches were encountered. Sometimes a discontinuity plane created for mapping a feature would translate to a random portion of the model or to an area entirely outside of the model. The orientation of the feature would remain as it was originally mapped, but the feature would not display at the correct location. Consequently, it was difficult to make sure that individual fracture surfaces were not being mapped in multiple instances. It was also found that the controls for rotating the model responded more effectively when using a portion of the point cloud, versus the whole point cloud. Since ContextCapture originally split the model into four sections, two were selected to use for mapping joint sets. Then, the data from both portions of the model were combined into a single stereonet.

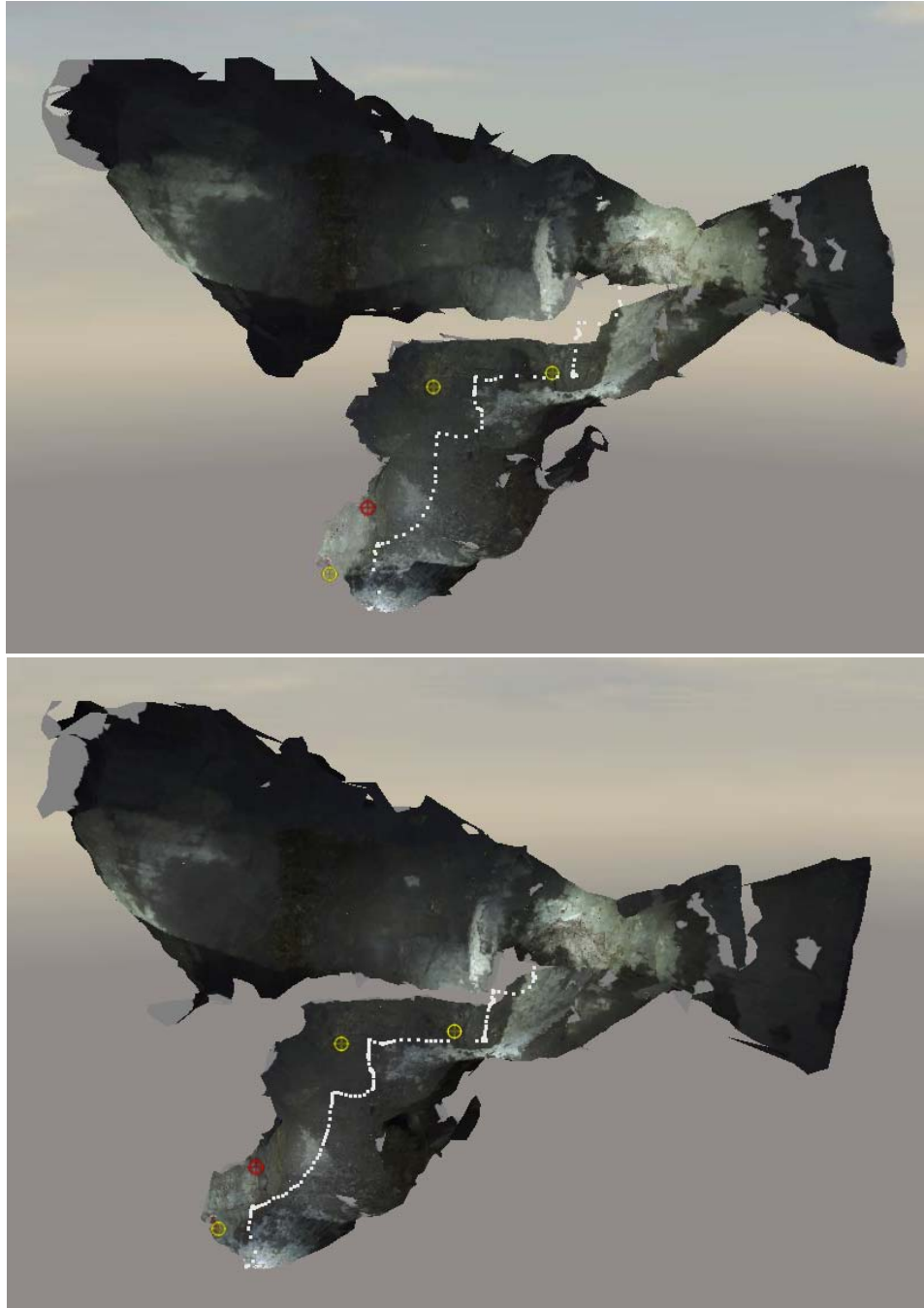


Figure 17. Bentley ContextCapture 3D models of the NEV Stope at GSM created from UAV imagery; the top image shows a model made with 225 stills and the bottom image shows the model made using 446 stills all extracted from the video imagery. The yellow dots show the locations of the measured ground control points used for constructing the model. The red dot is a control point that was measured, but not used for constructing the model.

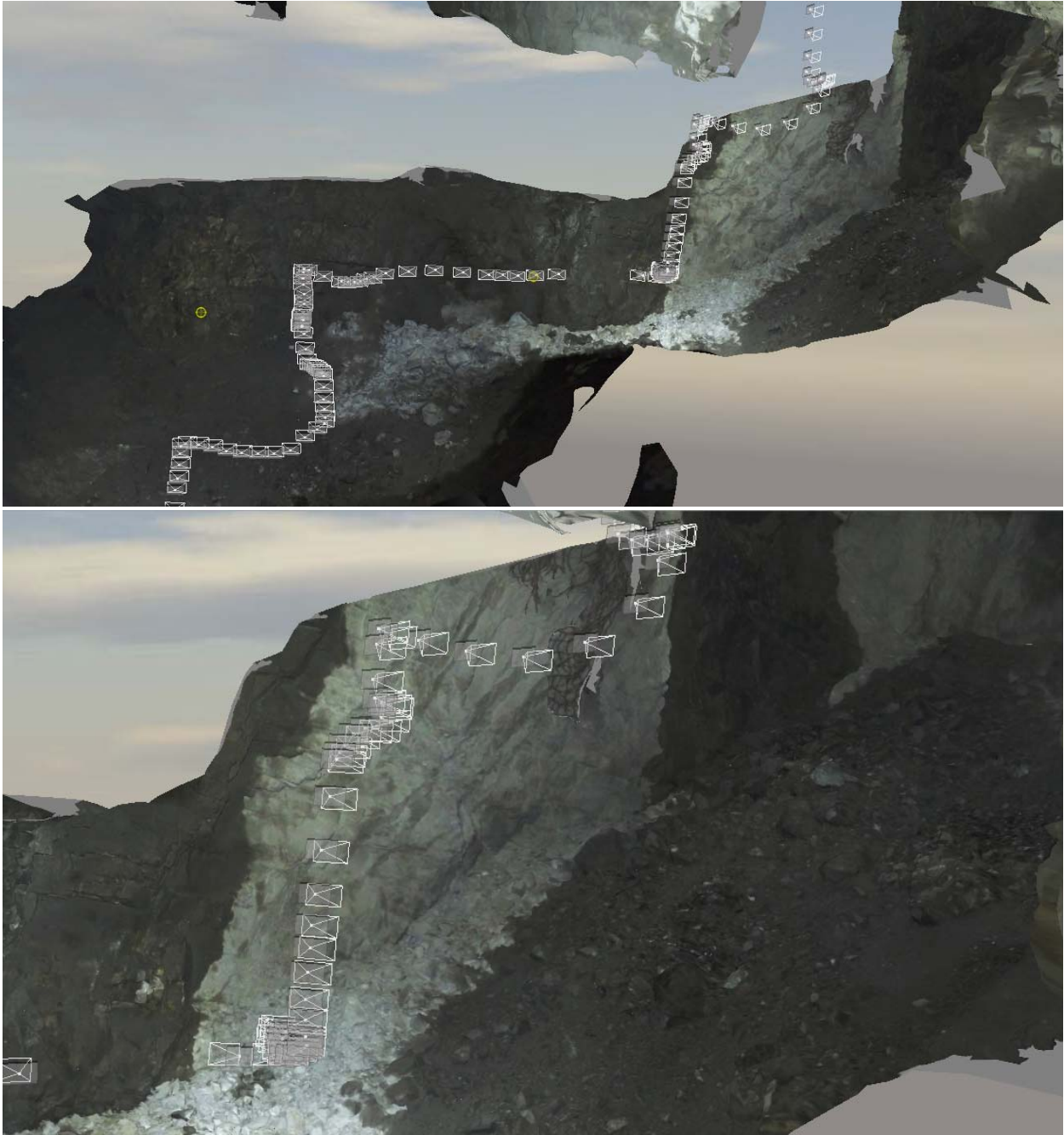


Figure 18. ContextCapture 3D stope model showing the camera locations (in white wireframe) in relation to the parts of the model that were captured and the parts that were not (the holes).

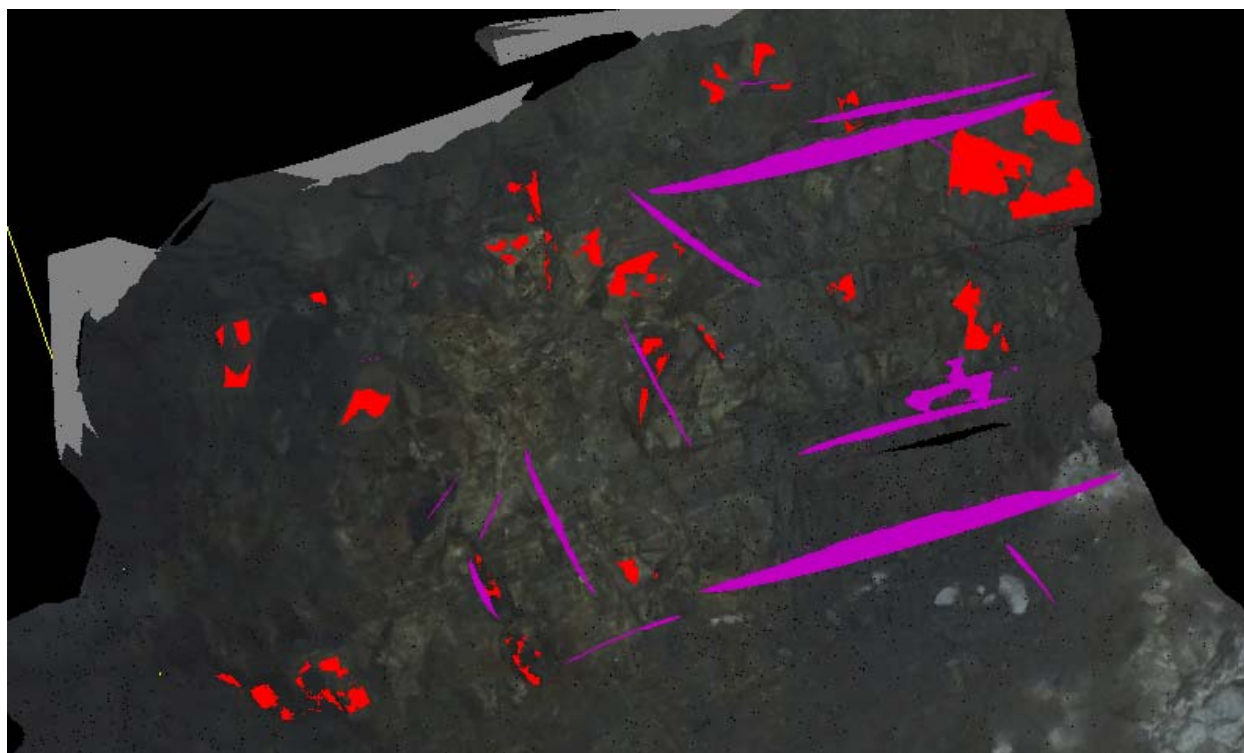


Figure 19. Two ContextCapture model tiles mapped using Split-FX: the location of some of the planes used for mapping the structures may not be located in the correct location on the model, but remain in the correct orientation due to a glitch within Split-FX.

Because mapping using Split-FX was not as user-friendly as mapping using 3DM Analyst, the 446 image model was exported from ContextCapture and loaded into 3DM Analyst for mapping. Figure 20 shows screen captures of the mapped stope joint sets using 3DM Analyst. Once the discontinuities were mapped, they were divided into sets through manipulation of the discontinuity planes within the stereonet. The different structural sets are delineated by corresponding color in the model and in the stereonet.

Prior to data collection, the rock surface of drawpoint 1 and the drift leading to drawpoint 1 of the NEV Stope were hand mapped using a dip/dip direction Brunton compass. Figure 21 shows the field mapped structural features measured in the drift leading to and the entrance of drawpoint 1. Using Rocscience Dips 7.0 software, the structures mapped in the field were manually entered into the software to create a stereonet of the discontinuity planes. Figure 22 shows the stereonet from mapping that was performed in the field compared to the stereonets from digital mapping carried out using Split-FX and 3DM Analyst in the portion of the NEV Stope closest to drawpoint 1. The two digitally mapped models allowed for identification of northeasterly striking structures that were not identified during field mapping.

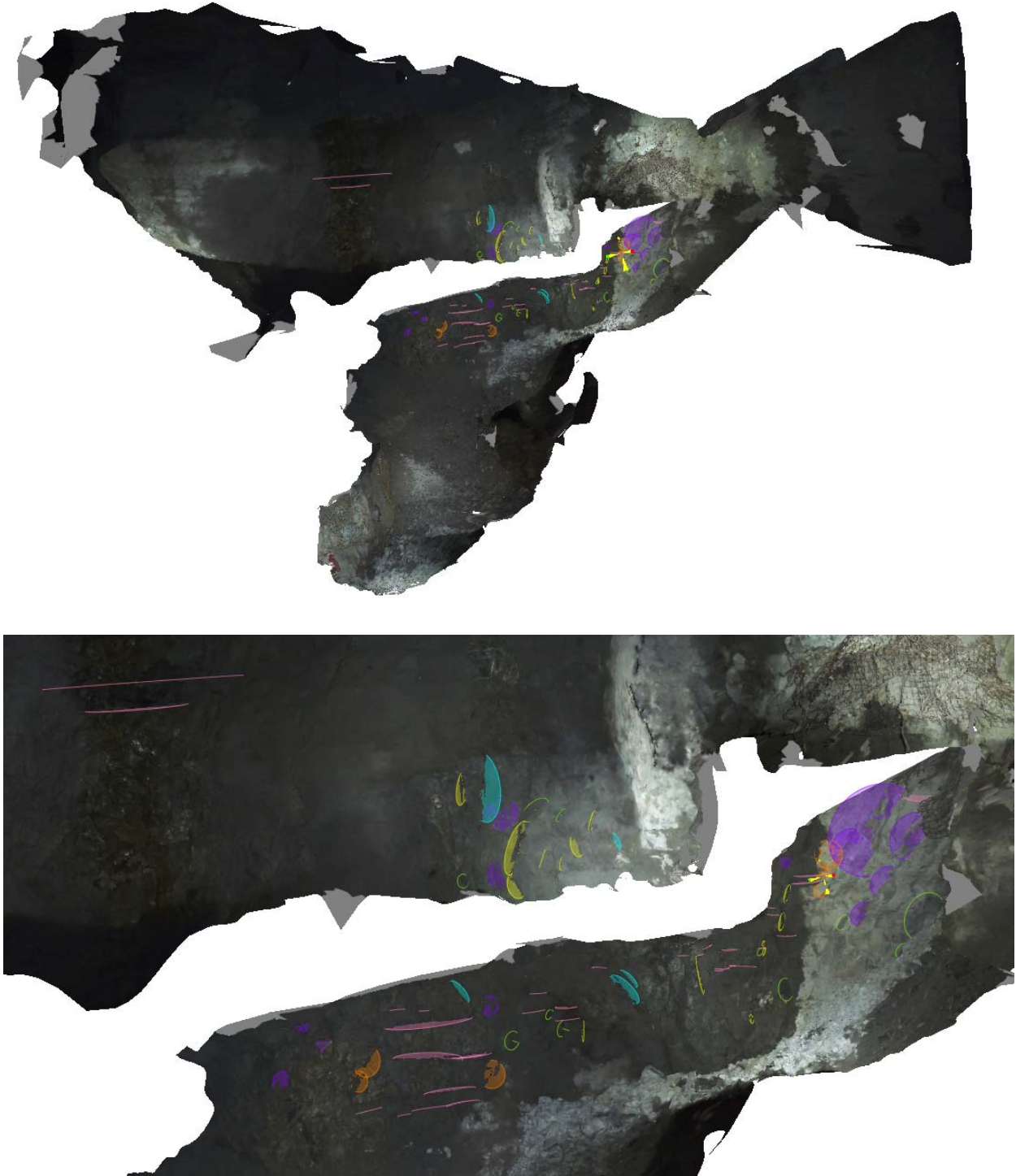


Figure 20. ContextCapture model mapped using 3DM Analyst with structural planes present within the NEV
Stope color-coded by orientation set.

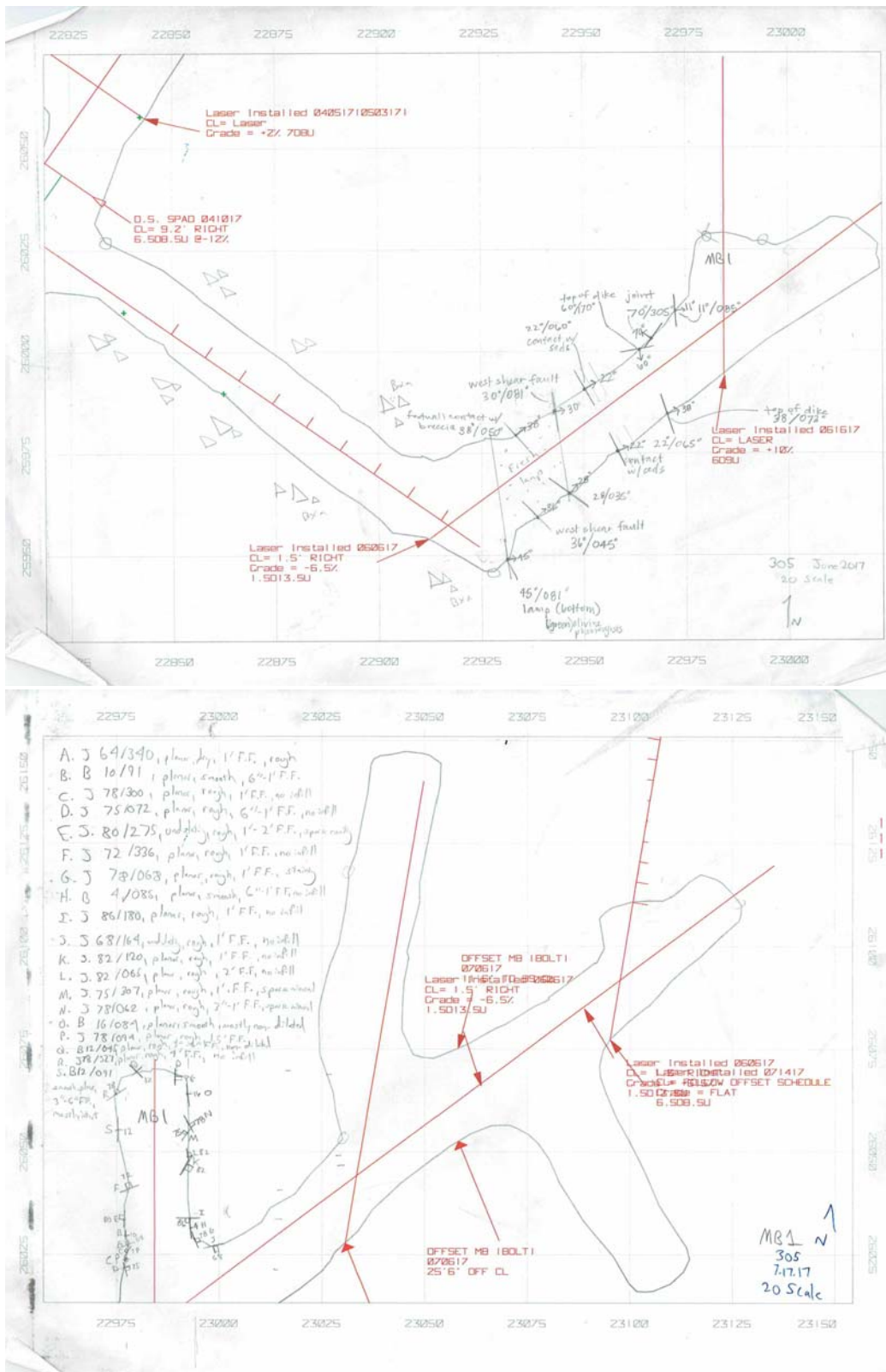


Figure 21. Hand mapped structure present in the drift leading to the stope drawpoint entrance (top) and within the first drawpoint entrance (bottom) (GSM mapping files).

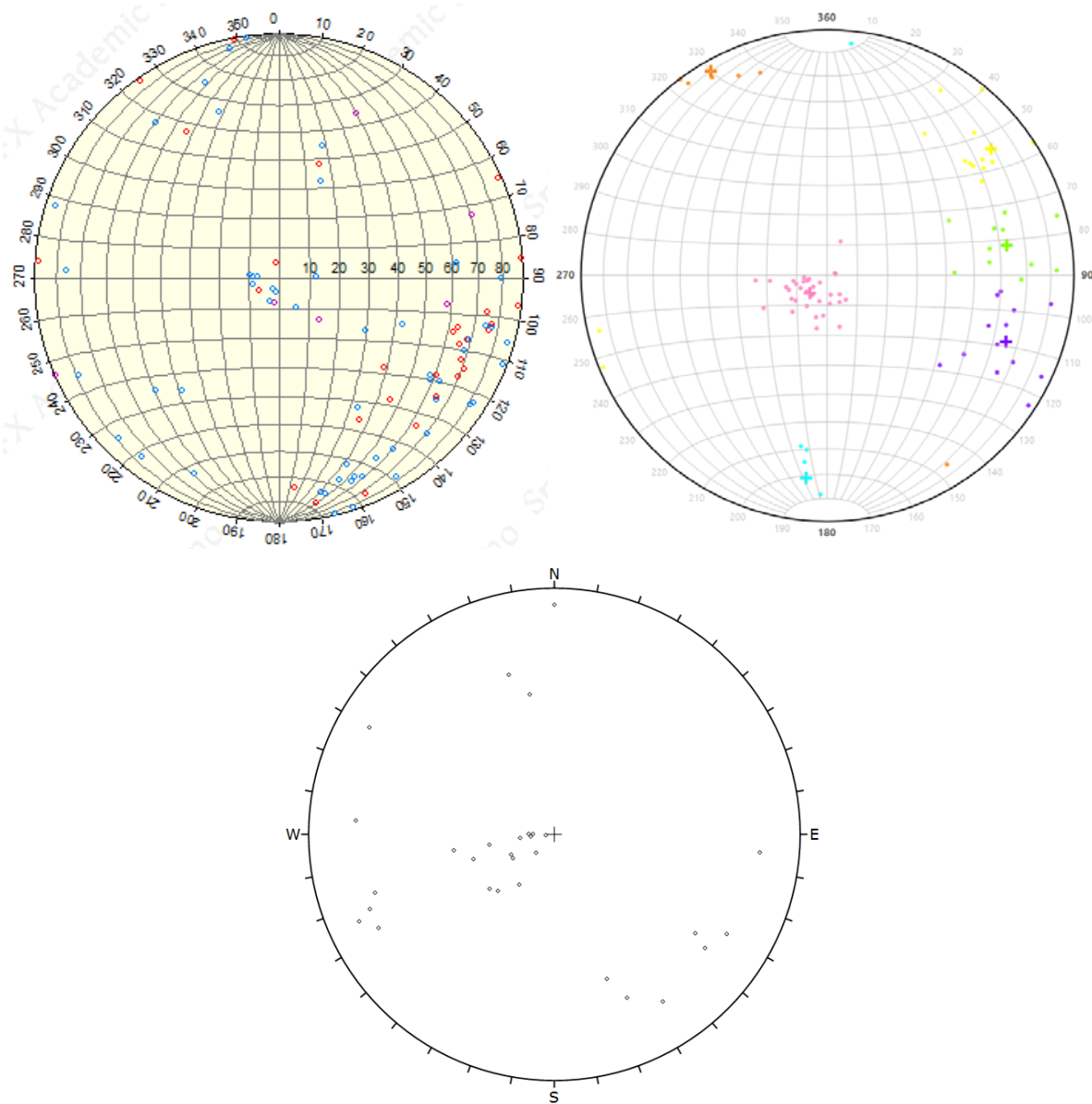


Figure 22. Stereonets (in equal area projection) of mapped joint sets in the NEV Stope and areas leading into the first drawpoint of the NEV Stope at GSM using Split-FX (*left*), 3DM Analyst (*right*), and hand mapping (*bottom*).

8. Conclusions and Recommendations

The aim of this project was to introduce a UAV-based digital photogrammetric system that is (preferably) a physically compact, off-the-shelf solution for underground geotechnical rock mass characterization. Several objectives needed to be achieved, including flying the UAV out of LOS, maintaining flight control, lighting the rock faces to produce enough light for the Guidance system to function at a distance while capturing quality imagery, georeferencing points within an inaccessible area, using the imagery to build 3D models, and mapping structures identified on the models. By accomplishing these goals, it was determined that using a UAV for capturing photogrammetry data in a stope via manual flight is a viable option for modeling and mapping structural features located within large open voids underground; thus, gaps in the geotechnical knowledge of the site can be filled to create a potentially safer mine.

When considering the platform used for capturing the underground photogrammetry data, the M100 served the purpose well. It was able to successfully capture imagery in an underground inaccessible stope. It was rugged enough to survive a crash underground, and needed very few repairs. The original UAV legs would not have likely survived the crash, so that is one downfall to the M100. Overall, the M100 was able to complete the task. More research into UAV obstacle detection and avoidance systems would facilitate successful underground flight in the future.

Two sets of software were used for the modeling and mapping aspects. When working with both software packages, it became apparent that the underground models are more reliably built using Bentley's ContextCapture, likely due to the fact that ADAM Technology was developed for carefully planned imagery capture locations. ContextCapture was straightforward to use and generated quality models that can be easily be navigated. ADAM Technology's suite of software for building the DTM is not as intuitive as ContextCapture and is less

straightforward regarding which steps to take. The ADAM Technology suite was designed for accurate data modeling captured from specific locations, but use of UAV-based imagery from manual flights (without GPS signal) does not allow for data collection at precisely specified locations. It is convenient, though, that the ADAM Technology suite integrates a program for mapping structural data. ContextCapture does not, so Split-FX was used for mapping the ContextCapture models. At this time, point clouds created by ContextCapture are not compatible with Split-FX input file formats, requiring conversion of the exported ContextCapture point clouds using Agisoft PhotoScan (or another software capable of the file format conversion). Mapping using Split-FX was much more difficult than mapping using 3DM Analyst. In Split-FX, the point cloud was slow to respond to manipulation using the mouse, including manual rotation and zooming. When trying to pull the model in a certain direction, the model was moved in a different direction. Lack of experience with the Split-FX software, as compared to 3DM Analyst, is likely contributable to these issues. In contrast, mapping features in 3DM Analyst was fairly easy to navigate, and the models were easily manipulated.

From the analyses performed for this study, it can be concluded that neither using ADAM Technology's software nor using Bentley's ContextCapture with Split Engineering's Split-FX is an optimal underground photogrammetric modeling and mapping software approach. Without an absolute orientation of the model (in the 895-102 drift), ContextCapture produced a more reliable model than 3DM CalibCam and the DTM Generator. Bentley's ContextCapture seems to be a more appropriate software for underground UAV photogrammetric model creation, because the locations of camera stations and the distance from the object being captured does not need to be specific, like in ADAM Technology. ContextCapture successfully built a model of the NEV Stope from which geotechnical data were collected. The joint sets identified compared well to

those established by manual mapping of nearby locations. Through the digital mapping, northeasterly striking discontinuities were identified that were not identified in field mapping. Using the geotechnical data collected in this project for kinematic analyses will provide insight into the stability of the stope walls. When manually mapping geotechnical data, though, ADAM Technology's 3DM Analyst is much easier and efficient.

No solution is perfect, but the data measured from the mapped models can potentially create a safer mine. Due to the presence of large stopes at GSM, it is critical to understand the rock mass and its inherent stability as completely as possible. With improvements in underground flight planning and data capture, 3D stope models created from UAV photogrammetry and geotechnical mapping of modeled features will fill in the geologic data gaps in inaccessible areas of mines.

One related immediate outgrowth of this research would be to evaluate the imagery based models in terms of their usability to determine the rock mass quality in inaccessible areas. Based on the ability to detect joint sets demonstrated via the NEV Stope imagery and model, the UAV will be able to capture enough data to form estimates of Q or RMR from measurements made in and observations of the model. For RMR, the degree of fracturing; the discontinuity spacing, condition, and orientation; and the groundwater conditions all have the potential to be derived from the model and/or video imagery collected in the stope. The uniaxial compressive strength of the intact rock is the only component of RMR that would not be able to be derived from the model, but values for the same rock types in the mine could be used for the estimate; this is routinely done to augment the standard field estimate of strength based on striking the rock with a geologic rock hammer. For an estimation of Q, the block size, joint alteration, joint water reduction factor, and stress reduction factor could likely all be estimated from the imagery. The

most difficult factor to estimate from imagery would be joint roughness, but again, this value could be estimated based upon known information about different rock types in the area.

Collecting the information needed to classify the rock mass according to these indices would provide data not only for more thorough kinematic analyses that will contribute to determining the stability of the rock mass exposed in the excavation, but also to designing excavations and their respective support.

General recommendations for future research include evaluating the performance of obstacle avoidance sensors in low light scenarios and using a UAV that is rated for exposure to dust and water. Specific recommendations are as follows:

- Flights should be planned based on the shape of void being imaged and the position of the UAV operator should maximize the LOS for all parts of the flight.
- Another possible step to be taken prior to the main data collection would be to use the UAV to scope out defining features located in different areas of the stope. This will allow the pilot to have a better idea of the UAV's position and orientation once it is out of LOS during data collection.
- Imaging should begin while the UAV is still low to the ground, initially focusing on capturing all data in front of and to the sides rather than in a spiral path. Then, the pilot should work on capturing data with the drone turned around 180° and up higher in the stope.
- In addition to the pilot, a separate remote controller should be used for more efficient data collection (e.g. for movement of the camera). The second remote controller, termed a "slave remote" could be used solely to control the camera, while the main pilot focuses on the manual flight. Clear communication between

the pilot and the person operating the slave remote controller will allow for much smoother and successful data collection.

As technology progresses, efficient algorithms will help to speed up the geotechnical analyses performed in underground mining, thus allowing for a greater efficiency in mining processes. UAV system automation would greatly improve the data collection process for collecting underground geotechnical data from areas that cannot be accessed.

While the focus of this project was using off-the-shelf technology available at a low cost, other technology was encountered that could enhance performance, but at substantially higher costs. Additional options to consider for improving data collection in the future include:

- using beacons to extend the range of communication between the UAV and remote controller(s),
- evaluating the performance of other UAV platforms (for instance, the Inkonova TILT Ranger UAV that may be customized to achieve the project goals, so that obstacle avoidance is not contingent upon the cooperation of the DJI Guidance system), and
- using a UAV LiDAR, SLAM, and/or a similar product in conjunction with a time-synchronized camera that combines the ability to generate a dense RGB point cloud with built-in obstacle avoidance and potential utilization of an autonomous flight path.

It is anticipated that using a LiDAR system with SLAM and a time-synchronized camera will be the most ideal data collection system. Using all of these technologies simultaneously will allow for a very dense point cloud (via LiDAR), obstacle detection/avoidance and autonomy (via SLAM), and more detailed data with the RGB values assigned to each point (via camera).

Multiple companies have accomplished different components of this ultimate underground

remote sensing tool, and with one or more robust, fully integrated systems available in the near future a tool that can dependably collect useful geotechnical data in inaccessible underground areas via UAV will be available. These companies are also focused on using autonomy for UAV data collection, which would greatly facilitate underground use of this powerful tool.

9. References Cited

100W LED Modules. (n.d.). Retrieved October, 2018, from

<https://www.stratusleds.com/module/>

ADAM Technology. (2010). 3DM Analyst Mine Mapping Suite 2.3.4 User's Manual. Revision 1.0.137.

ADAM Technology. (2018). *About us*. Retrieved May 04, 2018, from

<https://www.adamtech.com.au/Company.html>

Atlas Copco. (2007). Sublevel open stoping method. Retrieved April 05, 2018, from

https://queensminedesign.miningexcellence.ca/index.php/Sub-level_open_stoping#cite_note-AtlasCopco-0

ARM LED. (n.d.). Retrieved February, 2018, from <https://www.stratusleds.com/arm-led/>

Azhari, F., Kiely, S., Sennersten, C., Lindley, C., Matuszak, M., & Hogwood, S. (2017). A comparison of sensors for underground void mapping by unmanned aerial vehicles, in *Underground Mining Technology 2017*, (Australian Centre for Geomechanics: Perth).

Becker, R. E., Galayda, L. J., & MacLaughlin, M. M. (2018) Digital photogrammetry software comparison for rock mass characterization, at the *52nd US Rock Mechanics/ Geomechanics Symposium* (ARMA, American Rock Mechanics Association: Seattle, June 17-20).

Bentley. (2018). *ContextCapture User Guide*. Retrieved March, 2018. Updated 19 January 2018.

Birch, J. (2006). Using 3DM Analyst Mine Mapping Suite for rock face characterisation.

[PowerPoint slides]. Retrieved from

<https://www.adamtech.com.au/Publications/0904%20Geotech%20Engineering%20ADAM%20Technology.pdf>

Birch, J. S. (2009). Using 3DM analyst mine mapping suite for slope stability – case studies, in *ACG Geotechnical Engineering for Open Pit Mines*, 17, 1-15.

Buy Zenmuse X3 Gimbal and Camera. (n.d.). Retrieved April 3, 2018, from https://store.dji.com/product/zenmuse-x3-gimbal-camera?site=brandsite&from=buy_now_bar

Coggan, J. S., Wetherelt, A., Gwynn, X. P., & Flynn, Z. N. (2007). Comparison of hand-mapping with remote data capture systems for effective rock mass characterisation, at the *11th Congress of the International Society for Rock Mechanics*, (Taylor & Francis Group: London).

Colomina, I. & Molina, P. (2014). Unmanned aerial systems for photogrammetry and remote sensing: a review. International Society for Photogrammetry and Remote Sensing, Inc. (*ISPRS*) *Journal of Photogrammetry and Remote Sensing*, 92, 79-97.

Dang, T. T. (2015). The use of photogrammetry in measuring geologic structures and creating a 3D model on exposed rock faces, in *Vietrock2015 an IRSM specialized conference*: Hanoi, Vietnam).

Delaloye, D., Hutchinson, J., and Diedrichs, M. (2012). Using terrestrial LiDAR for tunnel deformation monitoring in circular tunnels and shafts, at the *Rock Engineering and Technology for Sustainable Underground Construction Eurock 2012*, (ISRM International Symposium, BeFo and IRSM: Stockholm, Sweden).

Donovan, J., & Ali, W. R. (2008). A change detection method for slope monitoring and identification of potential rockfall using three-dimensional imaging, at the *42nd US Rock Mechanics Symposium*, (ARMA, American Rock Mechanics Association: San Francisco).

- Donovan, J., & Lebaron, A. (2009). A comparison of photogrammetry and laser scanning for the purpose of automated rock mass characterization, at the *43rd US Rock Mechanics Symposium*, (ARMA, American Rock Mechanics Association: Asheville).
- DJI Guidance User Manual. version 1.6. (2015). *DJI GUIDANCE User Manual*. DJI, Shenzhen, Guangdong. Copy in possession of Montana Tech.
- DJI Inspire 1 User Manual(EN). version 2.0. (2016). *DJI Inspire 1*. DJI, Shenzhen, Guangdong. Copy in possession of Montana Tech.
- DJI Matrice 100 User Manual version 1.6. (2016). *DJI Matrice 100*. DJI, Shenzhen, Guangdong, China. Copy in possession of Montana Tech.
- Phantom 4 Pro - Professional aerial filmmaking made easy. (n.d.). Retrieved April 01, 2018, from <https://www.dji.com/phantom-4-pro>
- DJI Phantom 4 Pro – Specs, FAQ, Tutorials and Downloads. (2018). Retrieved March 27, 2018, from <https://www.dji.com/phantom-4-pro/info#specs>
- DJI Phantom 4 Pro/Pro+ User Manual. version 1.4. (2017). *DJI Phantom 4 Pro*. DJI, Shenzhen, Guangdong. Copy in possession of Montana Tech.
- DJI - The World Leader in Camera Drones/Quadcopters for Aerial Photography. (n.d.). Retrieved April 3, 2018, from <https://www.dji.com/matrice100/info#specs>
- Gaich, A., Potsch, M., & Schubert, W. (2007). Rock mass characterisation for tunnelling and mining using 3d images, at the *Rock Engineering and Technology for Sustainable Underground Construction Eurock 2012*, (ISRM International Symposium, BeFo and IRSM: Stockholm, Sweden).
- Gaich, A., Lenz, G., Wagner, P., Pötsch, M., Henzinger, M. R., & Schubert, W. (2015). Circular 3D images from TBMs, at the *11th Congress of the International Society for Rock*

- Mechanics*, (Taylor & Francis Group: London).
- Greenwood, W., Zekkos, D., Lynch, J., Bateman, J., Clark, M. K., & Chamlagain, D. (2016). UAV-based 3-D characterization of rock masses and rock slides in Nepal, at the 50th US *Rock Mechanics Symposium*, (ARMA, American Rock Mechanics Association: Houston).
- Haines, O. (2016, May 13). An introduction to simultaneous localization and mapping [web log comment]. Retrieved on May 2, 2018, from <https://www.kudan.eu/kudan-news/an-introduction-to-slam/>
- Hamrin, H. (2001). Underground mining methods and applications. In W. A. Hustrulid & R. L. Bullock (Eds.), *Underground Mining Methods: Engineering Fundamentals and International Case Studies* (p. 7). Society for Mining, Metallurgy, and Exploration.
- Hoek, E., Kaiser, P. K., & Bawden, W. F. (1995). *Support of underground excavations in hard rock*. Rotterdam, Netherlands: A.A. Balkema.
- Hoek, E. (2007). *Practical rock engineering*. Retrieved from <https://www.rocscience.com/learning/hoek-s-corner/books>
- Kottenstette, J. T. (2005). Measurement of geologic features using close range terrestrial photogrammetry, at the 40th US *Symposium on Rock Mechanics (USRMS)*: Anchorage, AK, June 25-29.
- Lato, M. J., & Vöge, M. (2012). Automated discontinuity orientation mapping from lidar data. *International Society for Rock Mechanics and Rock Engineering*, (ISRM International Symposium: Stockholm, Sweden, May 28-30).

- Levy, M. E. & Visca, P. J. (2009). *43rd US Rock Mechanics Symposium and 4th U.S.-Canada Rock Mechanics Symposium*. (ARMA American Rock Mechanics Association: Asheville, NC, June 28 – July 1).
- Light Cube Spotlight Headlight Kit for DJI Inspire 1 2 Matrice 100 200 (Listing for 1 Light). (n.d.). Retrieved October 22, 2017, from [https://www.firehousetechnology.com/store/p42/Light_Cube_Spotlight_Headlight_Kit_for_DJI_Inspire_1_2_Matrice_100_200_\(Listing_for_1_Light\).html](https://www.firehousetechnology.com/store/p42/Light_Cube_Spotlight_Headlight_Kit_for_DJI_Inspire_1_2_Matrice_100_200_(Listing_for_1_Light).html)
- Lingen, J. (2011). *Digital camera calibration for mining applications* Retrieved from Education and Research Archive (ERA) Digital Thesis. 10.7939/R3707P
- Liu, Q., & Kieffer, D. S. (2012). Digital tunnel mapping using terrestrial LiDAR - a case study. *International Society for Rock Mechanics and Rock Engineering*: Stockholm, Sweden.
- Liu, Q. (2013). Remote sensing technologies in rock mass characterization. In X. Feng, J. A. Hudson, & F. Tan (Eds.), *Rock Characterisation, Modelling and Engineering Design Methods* (pp. 205-210). London: Taylor and Francis Group.
- Lume Cube - Single (Black). (n.d.). Retrieved September, 2017, from <https://www.lumecube.com/shop/single-lume-cube>
- Mathis, J. I. (1987). Discontinuity mapping – A comparison between line and area mapping, at the *6th International Society of Rock Mechanics and Rock Engineering Symposium (ISRM)*: Montreal, Canada, Aug. 30-Sept. 3.
- National Institute of Safety and Health (NIOSH). (2017). [Bar graph illustration of numbers and percentages 2011-2015]. *Number and percentage of occupational fatalities by accident class: underground mining locations, 2011-2015 (N=75)*. Retrieved April, 2018, from <https://www.cdc.gov/niosh/mining/statistics/allmining.html>

- Onboard SDK. (n.d.). Retrieved April 4, 2018, from <https://developer.dji.com/onboard-sdk/documentation/guides/component-guide-flight-control.html>
- Otoo, J. N., Maerz, N. H., Xiaoling, & L., Duan, Y. (2011) 3-D discontinuity orientations using combined optical imaging and LiDAR techniques, at the *45th US Rock Mechanics/Geomechanics Symposium*. (ARMA American Rock Mechanics Association: San Francisco, CA, June 26-29).
- Rees, K, 2012. The benefits of using photogrammetry in the geological interpretation of the cosmos nickel mine, in *Proceedings Narrow Vein Mining 2012*, (The Australasian Institute of Mining and Metallurgy: Melbourne).
- Remondino, F., Barazzetti, L., Nex, F., Scaioni M., & Sarazzi, D. (2011). UAV photogrammetry for mapping and 3D modeling – current status and future perspectives. *International Archives of the Photogrammetry, Remote Sensing and Spatial Information Sciences*, 38. Retrieved from http://3dom.fbk.eu/sites/3dom.fbk.eu/files/pdf/Remondino_etal_UAV2011.pdf
- Sub-level open stoping. (n.d.). Retrieved April 04, 2018, from https://queensminedesign.miningexcellence.ca/index.php/Sub-level_open_stoping#cite_note-AtlasCopco-0
- Styles, T. D., Zhang, Y., Stead, D., Elmo, D., Roberts, D., & Yanske, T. (2010). A photogrammetric approach to brittle fracture characterization in mine pillars, at the *44th US Rock Mechanics Symposium*, (ARMA, American Rock Mechanics Association: Salt Lake City).
- Tamburini, A., Martelli, D. C. G., Alberto, W., & Villa, F. (2015). Geomechanical rock mass characterization with terrestrial laser scanning and UAV, at the *49th US Rock Mechanics*

- Symposium*, (ARMA, American Rock Mechanics Association: San Francisco).
- Terzaghi, K. (1942) Shield tunnels for Chicago subway. *Boston Society of Civil Engineers*, 29 (3), 163-210.
- Tonon, F. & Kottenstette J. T. (2006). Summary paper on the Morrison field exercise. In F. Tonon & J. Kottenstette (Eds.), *Laser and photogrammetric methods for rock face characterization* (pp. 77-96). Golden, Colorado: ARMA.
- Turner, R. M., Bhagwat, N. P., Galayda, L. J., Knoll, C. S., MacLaughlin, M. M., Russell, E. A. (2108). Geotechnical characterization of underground mine excavations from UAV-generated photogrammetric and thermal imagery, in *Proceedings of the 52nd US Rock Mechanics/Geomechanics Symposium*. (ARMA American Rock Mechanics Association: Seattle, 17-20 June 2018).
- Vallejo L. I. G., & Ferrer M. (2011). *Geological engineering*. London: Taylor & Francis.
- Wu, R. (2017). *Test of GeoSLAM at range front decline and its potential application [PowerPoint Slides]*. Presented on 02 November 2017 at the Annual Geomechanics and Hydrogeology (GHG) Conference and Annual Meeting in Elko, Nevada.
- Zenmuse X3 - Creativity Unleashed. (n.d.). Retrieved September, 2017, from <https://www.dji.com/zenmuse-x3/info>
- Zlot, R., & Bosse, M. (2014). Efficient large-scale three-dimensional mobile mapping for underground mines. *Journal of Field Robotics*, 31(5), 758-779. doi:10.1002/rob.21504

10. Appendix A: UAV Systems

This appendix contains supplemental specifications on the DJI Phantom 4 Pro and the DJI Matrice 100 UAVs not listed in the main text. Specifications on both UAV's added features are also included.

10.1. DJI Phantom 4 Pro

All built-in features of the P4P system communicate with the flight controller to allow for successful data collection, settings adjustments, a real-time view from the UAV camera, among other functions (DJI Phantom 4 Pro/Pro+ User Manual, 2017). The advanced features of the system are referred to the aerial system's "FlightAutonomy." A battery, remote controller, charger for the battery and remote controller, and propellers are all also included in the box, so that the system is "ready-to-fly" once a few simple steps are taken to prepare the UAV for flight:

- Charge the battery and remote controller,
- Check the firmware for updates (and updated if necessary), and
- Calibrate the obstacle sensing system, IMU and compass (Onboard SDK, n.d. & DJI Phantom 4 Pro/Pro+ User Manual, 2017).

10.1.1. Compasses and IMUs

For the UAV to remain stable while hovering and during flight, the compasses and IMUs are included in the P4P system. The dual IMUs and compasses included in the P4P measure the UAV speed and directional data, to create a more stable and reliable platform. The compass uses "dual-band satellite positioning (GPS and GLONASS)" (DJI Phantom 4 Pro-Specs, 2018). It helps to determine the direction of flight relative to its measurement of magnetic North (Onboard SDK, n.d.). The IMUs each contain an accelerometer and a gyroscope for measuring the linear acceleration and angular velocity of the aircraft during flight. At times, both the IMUs and compasses will need to be calibrated, which will be indicated by the aircraft status indicator (an

LED on the back of the UAV) and on the DJI GO 4 app. The UAV must be calibrated before it will allow the UAV to fly.

10.1.2. Flight Modes

Three flight modes are available to choose from on the P4P aircraft: P-mode, S-mode, and A-mode (DJI Phantom 4 Pro/Pro+ User Manual, 2017). P-mode stands for positioning mode and functions ideally when GPS-signal is strong; however, when in P-mode, the UAV automatically toggles between different states depending upon the strength of the GPS signal (or if GPS is available). In P-mode the UAV simultaneously uses the obstacle sensing system to stabilize the UAV while avoiding obstacles. If or when GPS signal is available, the UAV will switch its state so that it only relies on GPS, while still functioning in P-mode. If the GPS-signal becomes weak or if low lighting conditions cause the obstacles sensing not to function while flying in P-mode, the aircraft will rely on its internal barometer for positioning. One advanced function in P-mode is Tripod Mode. Using Tripod Mode enables the side sensors of the UAV, but does not allow very fast flight speeds. Tripod Mode was useful when flying in small confined areas. Other advanced features not pertaining to the scope of this project can also be enabled in P-mode. When both obstacle sensing and GPS-signal are unavailable, A-mode, or Attitude mode, can be selected so that the UAV uses its barometer for positioning and altitude. Sport mode (S-mode) can be set if the operator would like to fly at speeds up to 72 kph (45 mph) with increased maneuverability, but a disabled obstacle sensing system.

10.1.3. Camera

A stock camera with a 1-inch type, 20-megapixel, CMOS (complementary metal oxide semiconductor) sensor (width: 13.2 mm x height: 8.8 mm) comes preinstalled on the P4P (Phantom 4 Pro/Pro+ User Manual, 2017). The 8.8 mm (24 mm equivalent of 35 mm format)

lens on the camera uses a mechanical shutter to eliminate imagery distortion. It has a wide-angle field-of-view of 84° and an f-stop range of 2.8-11. The camera's autofocus ranges from 1 m to infinity. The ISO ranges vary between video and photo format and between automatic and manual shooting. For both videos and photos shot in the automatic setting, the camera ISO can range from 100-3200. When shooting in the manual setting, the ISO range can be set to range between 100-6400 when capturing a video and 100-12800 when capturing photos. Photo file types include JPEG, DNG (RAW), JPEG + DNG, while video file type options are MOV or MP4. Photo shooting modes for the P4P camera, include single, burst, auto-exposure bracketing (AEB), time-lapse/interval; the video modes are C4K, 4K, 2.7K, FHD, and HD. The maximum resolution that the photos can be captured in is Cinema 4096 x 2160 (C4K). For video, the maximum resolution of imagery capture is 4096 x 2160 (4K) at 60 frames-per-second (fps) and with a maximum video bit rate of 100 Megabits-per-second (Mbps). A real-time preview of what the camera sees can be observed in the DJI GO 4 application through a connected mobile device or tablet style device. The connected device stores a reduced quality version of the imagery captured, and the full-sized imagery is stored on a micro-USB that connects to the aircraft. For stability and smoother shooting, a three-axis gimbal (pitch, roll, and yaw) is attached to the camera allowing it 120 degrees of total vertical tilt. Modes locking the gimbal in the forward direction or in first-person view can be toggled on and off in the DJI GO 4 app as well.

10.1.4. Obstacle Sensing and Avoidance

Obstacle sensing and avoidance on-board the P4P aerial platform is comprised of dual vision sensors in the front, rear, and downward directions and 3D infrared scanners on the left and right sides of the aircraft (Phantom 4 Pro/Pro+ User Manual, 2017). Two ultrasonic sensors located on the underside of the UAV also assist the downward facing sensors in detecting the

ground and maintaining position. The front and rear visual sensors are stereo cameras located on Figure 23 the aircraft legs. The 3D infrared scanners are located on the sides of the body of the aircraft.



Figure 23. DJI Phantom 4 Pro obstacle sensor locations (Phantom 4 Pro/Pro+ User Manual, 2017): rear [1], front [2], and downward [3] cameras used for positioning, downward ultrasonic sensor [4], and 3D infrared sensor [5].

Obstacles that are sensed in the front, in the rear, and on the sides of the UAV are avoided at a user defined distance, set during calibration. The vision system sensing range can be set to avoid obstacles 0.7 to 30 m (2 to 98 ft.) away from the UAV. While Phantom 4 Pro-Specs (2018) specifies that the vision system requires an operating environment with surfaces with clear patterns and adequate lighting greater than 15 lux, the Phantom 4 Pro/Pro+ User Manual (2017) states that the lux must be greater than 10 and less than 10,000. Additionally, for the many of the other intelligence features to function, the lux must be greater than 300. Even when utilizing all the sensors, the UAV still possesses blind spots, where obstacles cannot be sensed. Figure 24 shows the ranges of the sensors and the blind spots where obstacles cannot be sensed.

On the sides of the aircraft, obstacle sensing and avoidance is only active if the UAV is flown in Beginner Mode (requiring GPS-signal) or Tripod Mode (limiting aircraft speeds) – two modes that can be selected separately within the DJI GO 4 app while in P-mode. Obstacles are

able to be sensed between 0.2 to 7 m (0.6 to 23 ft.) away from the UAV if the surface of the obstacle is a diffuse reflection material with a reflectivity less than 8%. Many other disclaimers such as flying over transparent, moving, or inclined surfaces, to name a few, are forewarned for sensing system functioning.

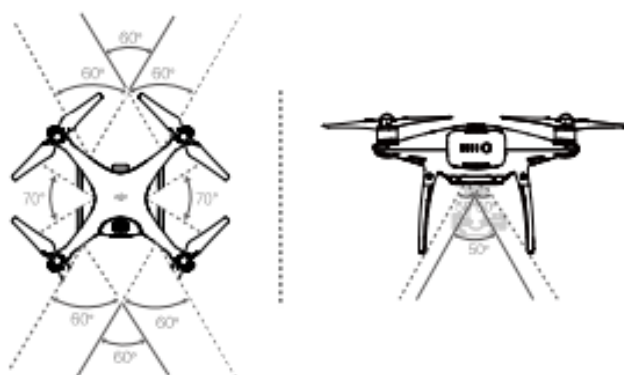


Figure 24. Ranges of obstacle detection sensors and associated blind spots on the DJI Phantom 4 Pro (DJI Phantom 4 Pro/Pro+ User Manual, 2017).

10.1.5. On-board Lighting Systems

Two lighting systems were tested (with minor adjustments between tests) on the P4P to determine whether they could provide enough light for quality imagery and for the obstacle sensing system to function properly. The two lighting systems that were tested are shown in Figure 25: the Lume Cubes were mounted on the P4P legs using a mounting kit designed specifically for the Lume Cubes, and the Firehouse Technology lights were mounted using the stock connectors.

The Lume Cube lights were chosen for testing because they are designed for rugged flying conditions and provide a significant lux for their respective weight. Each cube has 10 settings of brightness ranging from 150-1500 lumens which can be set through a mobile device with Bluetooth and the app Lume-X (Lume Cube - Single (Black), n.d.). The app can also be

used to make the lights flash for photography versus leaving them on with a constant light beam. Another option though is to adjust the brightness setting of each light manually. At 50% brightness, one Lume Cubes lasts over 2 hours, and they are rechargeable via USB cable. The light color temperature of the Lume Cubes is in the range of daylight at 6000 K, which is preferable for lighting a rock face. Each Lume Cube is about 1.5 in³ (24.6 cm³) in size and weighs about 3.5 ounces (99.2 grams).



Figure 25. *Left:* Lume Cube lights attached to P4P for testing, *Right:* Firehouse Technology lights used for testing on-board the P4P.

As an alternative, the Firehouse Technology UAV lights were tested since they are a more luminous and lighter weight option. Each light is made up of a panel of small 6000 K LEDs that have a total brightness of 1600 lumens (Light Cube Spotlight, n.d.). Each light stores a small rechargeable battery. One light is about 2 in³ (32.8 cm³) in size and weighs about 2.5 ounces (70.9 grams).

10.2. DJI Matrice 100

After assembling the M100, it is “ready-to-fly” after a few simple steps are taken to prepare for flight:

- Charge the battery and remote controller,
- Check the firmware for updates (and updated if necessary), and

- Calibrate the IMU and compass (DJI Matrice 100 User Manual, 2016; DJI - The World Leader, n.d.).

10.2.1. Compass and IMU

The M100 comes equipped with an IMU built into the flight controller and a mountable compass (DJI Matrice 100 User Manual, 2016). The systems function to measure the speed and direction of the M100, just as they function for the P4P (DJI Matrice 100 User Manual, 2016). The compass must be calibrated when indicated by the DJI GO application or the flight status indicator. Additionally, the compass should be calibrated for each new flight location. IMU errors are indicated using the same functions, and must be recalibrated on occasion as well. For ease of transport, the compass stand is able to fold down flat against the UAV body. When flying, it is important to make sure that the compass is in the upright position and that the arrow on the compass is facing toward the front of the aircraft.

10.2.2. Flight Modes

There are three options on the M100 for flight mode settings (DJI Matrice 100 User Manual, 2016). The flight mode determines whether or not GPS signal, the obstacle detection system, the barometer, or a combination of these will be used for controlling the positioning, maneuverability, and altitude of the aircraft. The M100 can operate in P-mode (positioning mode), A-mode (Attitude mode), or F-mode (function mode). There are three states located within the P-mode: P-GPS, P-OPTI, and P-ATTI. P-GPS mode uses GPS for positioning when it is available. When GPS is not available and the area where flight is occurring is well lit, the DJI Guidance system is used for positioning the UAV. If neither GPS-signal is available nor is the Guidance system (e.g. possibly due to low-light conditions or if it is not connected), then the aircraft toggles to P-ATTI mode. In this case, only the barometer is used for maintaining the UAV's altitude. A-mode can be set as the defined flight mode when GPS signal is not used for

positioning or is unavailable. P-mode ideally operates in an environment where GPS-signal is strong; however, if that is not the case, the M100 will automatically toggle into a different P-mode state, so that the aircraft can continue to operate properly in the current conditions. Like in the P-ATTI state, the UAV uses the barometer for maintaining altitude, but in A-mode the UAV has the capability of automatically returning to the home position if the remote controller signal is lost and if following conditions are met: the M100 is still receiving GPS-signal and the “home point” (starting point) was recorded successfully. To record the home point, GPS-signal must be available. The “RTH” button on the remote controller allows the operator to instruct the UAV to return to its starting point. F-mode is the third flight mode of the M100. F-mode supports special functions like Intelligent Orientation Control (IOC), which allows the operator to lock the nose direction of the UAV flight path. The special functions do not pertain to the research being conducted, but are described in the Matrice 100 User Manual (2017) in more detail.

10.2.3. Camera

The DJI Zenmuse X3 has a 1/2.3-inch type, 12.4-megapixel, CMOS sensor (width: 6.17 mm x height: 4.55 mm) (Zenmuse X3 – Creativity Unleashed, n.d.). The camera has a 3.6 mm (20 mm equivalent of 35 mm format) lens with a rectilinear, curved design that helps to eliminate lens distortion, like the fish-eye effect (Buy Zenmuse X3, n.d.); however, the rolling shutter does introduce a degree of distortion into the imagery. The lens has a 94° wide-angle field-of-view and f-stop of 2.8 at a focus range up to infinity. The ISO range can be adjusted, manually or automatically, between 100-3200. The camera is necessary for flight with the DJI Guidance System. Photo file types include JPEG and DNG, while video file type options are MOV or MP4. Shooting modes for capturing photos using the Zenmuse X3 camera, include single, burst, auto-exposure bracketing (AEB), and time-lapse/interval; the camera video modes

include 4K, FHD, HD (Inspire 1 User Manual(EN), 2017). The maximum resolution that the photos can be captured in is 4096 x 2160 (4K). For video, the maximum resolution of imagery capture is 4096 x 2160 (4K) at 24 frames-per-second (fps) and with a maximum video bit rate of 60 Megabits-per-second (Mbps).

10.2.4. DJI Guidance System

The Guidance system requires calibration upon first use. To calibrate the Guidance cameras, a desktop PC computer is needed and the DJI Guidance Assistant software is used. When calibrating the sensors, the distance at which the sensors are to be calibrated is defined. An LED indicator, present on each sensor and the Guidance core, flashes a specific color depending upon the status of the Guidance system. Figure 3 shows the location of the LED indicator on a sensor.

10.2.5. On-board Lighting Systems

The Stratus ARM LED components consist of a 100W 13,000 lumen 5600K 90 CRI LED emitter, an aluminum heat sink for the ARM LED, a 100W LED driver, and a 6S LIPO battery. They are designed to attach to the arms of a UAV (ARM LED, n/d.) and to serve as a light payload for UAVs, especially by relying on the UAV propeller wash for cooling the LEDs. The heat sink extends so that it can easily be attached to a UAV arm. Each 100W LED Module consists of the similar components as the ARM LEDs, including a 100W 13,000 lumen 5600K 85 CRI LED emitter, an aluminum heat sink for LED, a 24 V fan with input voltage range of 16-27 V, a 100W LED driver V2, a parabolic reflector, and a 6S LIPO battery (100W LED Modules, n.d.). The parabolic reflector focuses the beam angle of the LED from 170° to 60°, creating a higher lux output and, of course, a more focused beam angle (personal

communication, Daniel Riley, January, 25, 2018). The parabolic reflector was only used for the downward facing light, but was used with both the 100W Modules and the ARM LEDs.

The two lights were attached to parallel arms of the UAV. One Firehouse Technology connector was also used to connect the downward facing light on the UAV arm for the ARM LED lighting system. Also, a parabolic reflector from the 100W LED Modules was used for the downward facing light. The forward facing light was connected to part of the forward facing Guidance sensor with bolt screws, washers, and nuts as seen in the bottom image in Figure 3. Aside from soldering tools and solder, all other supplies (wires, power connectors, switches, and screws) were included in the assembly kit for both systems. An air-dry rubber coating called Plasti Dip was used to coat the LED drivers to protect them from damage due to moisture in the mine.

Because the downward facing light has a 100 mm (4 in.) parabolic reflector attached, the M100's stock legs were too short to be used with the Stratus LED lighting systems; thus, custom carbon fiber legs were designed and constructed using automobile oil drain plugs to create the connectors to attach the legs to the UAV as an alternative. The legs were designed not only to be longer than the stock legs, but also to be stronger than the plastic M100 legs. Carbon fiber tubes, with the same inner diameter (10 mm) and outer diameter (12 mm) as the stock legs were used for the main portion of the longer legs. The automobile oil drain plugs (M12-1.75) were machined into parts resembling the original leg connectors. The legs were attached to the connectors with epoxy and screwed into the M100 arms. Figure 26 shows what the drain plug looked like before and after being machined into the connector that is glued to the carbon fiber leg.



Figure 26. Before (*left*) and after (*right*) photos of one of the automobile drain plugs that was machined to create customized UAV leg connectors for the M100.

11. Appendix B: Flight Procedures

This appendix contains supplemental specifications on the calibrations and flight procedures followed for indoor, outdoor, and underground UAV flights.

11.1. Calibrating the Compasses and IMUs

The compasses and IMUs on board the UAVs need to be recalibrated on occasion, specifically when the UAV status indicator or the DJI GO (4) app indicates that a calibration is necessary (DJI Matrice 100 User Manual, 2017). Another scenario in which calibration is needed is after a significant crash. The calibration methods for the M100 and the P4P are the same except the M100 uses the DJI GO app, and the P4P uses the DJI GO 4 app for all UAV flight settings. When the compass(es) needs to be recalibrated the UAV status indicator, an LED light on the back of the UAV, alternates flashing red and yellow. If there is an IMU error, then the light will flash red only. Correcting IMU errors only requires placing the UAV on a level surface and navigating to the MC sensor settings in the DJI GO (4) app where there is a button for IMU calibration. Contrastingly, to recalibrate the compass(es), more interactive steps must be taken. First, the area chosen for calibration must be open, free of strong magnetic interference, including steel mesh used for support underground, and rid of cell phones due to ferromagnetic materials contained in them. If strong interference is still affecting the compasses after calibration, then the app will notify the operator with a warning and instructions for correcting the problem. Figure 27 depicts the two 360°-rotations that the UAV must complete to calibrate the compass(es). Sometimes the 360°-rotations must be continually repeated, in order for the UAV to calibrate the compass(es) successfully.

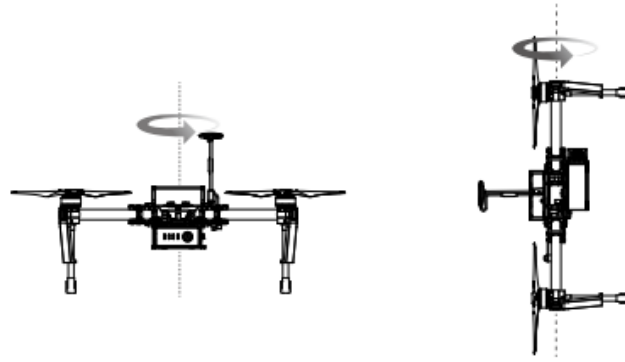


Figure 27. UAV compass calibration diagram showing the positions of the rotational axes and directions in which the system must be rotated for the calibration to be successful (DJI Matrice 100 User Manual, 2017).

11.2. Calibrating the DJI Guidance System

The steps taken to calibrate the DJI Guidance before performing tests are as follows:

- measure and record (in the app) the distance between each individual sensor and the center of the UAV body
- check each camera to ensure that it is functioning properly
- start calibration for a sensor
- face the sensor being calibrated toward the computer screen and a circle will appear on the screen with respect to the UAV
- follow the moving “o” shape on the screen with the circle that the sensor is projecting on the screen until notified to stop
- repeat the previous three steps for each sensor, until each one is calibrated
- close app and turn off UAV

With the Guidance cameras calibrated, four checks were performed before testing the

Guidance in flight:

- with the UAV connected to the remote controller, check to make sure that the distance at which the system was calibrated for is the distance selected in the DJI GO app
- check to make sure obstacle detecting is selected in the DJI GO app
- ensure the remote controller is in P-mode
- check that each sensor LED is green (confirms that hardware and software are performing as intended)

After all items were checked, the following steps were taken to conduct the testing procedure:

- take off in an area clear of obstacles (at a distance from obstacles greater than at the calibrated avoidance distance)
- ensure stable flight, and proceed to testing Guidance by attempting to fly at a range from the obstacle that is less than what was specified for obstacle detection (note: be sure to approach the obstacle such that it is not located within any of the system's blind spots)
- check to see if the system is providing warnings when approaching obstacles
- continue to test the sensors in all other directions and with detecting different types of obstacles
- land UAV and shut down system

11.3. Indoor Flights

When flying indoors, a series of steps specific to indoor flight were performed, so that the flight was carried out smoothly and safely. The following steps were taken in order each time the UAV was flown indoors.

- ask permission to fly in indoor area (clear of people)
- gather safety glasses for each person involved
- post signs at all entrances/exits into flight area
- have people watch/guard doors
- assign one person to video flights using phone or iPad
- clear area of objects that are in the way of flight path
- attach propellers to UAV (and optional propeller guards) – check to see if loose
- check that a memory card is inserted into the UAV (P4P)/camera (M100)
- insert battery into UAV and turn on
- connect battery for lights
- turn on remote controller
- connect to UAV through DJI GO (4) application on mobile device
- check that all settings are appropriate for intended flight goals
- check that remote controller is switched to the preferred flight mode
- check that everyone is prepared and wearing safety glasses
- turn on lights
- start UAV video
- fly/perform tests
- end video
- turn off UAV lights and remove light battery
- turn off and remove UAV battery (placing it in a fire-proof battery box)
- turn off remote controller
- pick up any trash off the ground (possibly broken propellers)
- return all items in area to original place
- take down signs

- pack up and leave site
- upload videos to UAV team's Sharepoint folder
- write summary of flight and upload it to Sharepoint folder

11.4. Outdoor Flights

Like for the indoor flights, a common procedure was followed each time an outdoor flight was conducted. These steps are listed below.

- find area that is not in FAA airport zone and obtain landowner permission to fly UAV
- ensure the flight procedure follows FAA regulations (https://www.faa.gov/uas/getting_started/)
- ensure area in which flight will take place can be accessed by foot if the UAV must be recovered and is clear of people and animals
- assign one person to video flights using phone or iPad
- attach propellers to UAV (and optional propeller guards) – check to see if loose
- check that a memory card is inserted into the UAV (P4P)/camera (M100)
- insert battery into UAV and turn on
- turn on remote controller
- connect to UAV through DJI GO (4) application on mobile device
- check that all settings are appropriate for intend flight reasons
- check that remote controller is switched to the preferred flight mode
- check that everyone is prepared for flight
- start UAV video
- fly/perform tests
- end video
- turn off and remove UAV battery (placing it in a fire-proof battery box)
- turn off remote controller
- pick up any trash off the ground (possibly broken propellers)
- pack up and leave site
- upload videos to Sharepoint folder
- write summary of flight and upload it to Sharepoint folder

11.5. Underground Flights

The steps taken for underground flights conducted at GSM are listed below. Underground flights conducted at the UMEC were carried out utilizing similar processes, except the georeferencing technique was not implemented and terrestrial lighting was used versus on-board lighting.

- arrive on mine site
- sign in
- load equipment in the mine truck (including the mine's total station, tripod, paintball gun, paintballs, and UAV box with UAV and all UAV accessories)
- gather personal protective equipment (PPE) required for entering an MSHA certified underground mine
- record underground survey point coordinates on plan view print out of area that will be mapped for resection (collected from Vulcan database for site)
- ride to mine portal entrance
- tag-in and sign-in
- load equipment into underground buggy or Minecat
- ride underground to site, while identifying escape ways along the way
- place flashing blue lights at beginning of drift to indicate foot-traffic (areas has already been cleared of heavy machinery)
- unload materials at site
- fill out 5-point card to assess working environment
- scale any loose material in the work area
- take UAV out of carrying case (need temperature to balance)
- take UAV camera out of case and attach to UAV
- let UAV system adjust to ambient temperature, wipe condensation from surfaces if necessary
- assign team member to take detailed notes
- assign team member to video flights using phone or iPad
- create control points (with paintball gun or spray paint) in the area where the UAV will be flown and within the LOS of the total station for resection
- identify locations of the survey points along the rib for resection
- set up total station in LOS of known survey points and area to be mapped
- perform resection to identify location of total station on the mine grid
- survey marked control points and take notes of the location and associated name of the GCP
- disassemble total station if obstructing flight area, otherwise wait until the flight is complete to disassemble in case the points cannot be captured by the UAV (may have to survey unmarked locations if less than 3 GCPs were captured in UAV video)
- lay out launching/landing pad for UAV and place UAV on top of it
- attach camera to UAV and make sure all camera lenses are clean
- attach propellers to UAV – check to see if loose
- check that a memory card is inserted into the camera
- insert UAV battery into UAV and turn on
- connect battery for lights
- turn on remote controller
- connect to UAV through DJI GO application on mobile device
- check that all settings are appropriate for intend flight reasons
- check that remote controller is switched to the preferred flight mode

- make sure that the guidance is working properly by checking that the small LED indicators on sensors are green (not flashing and not red)
- make sure that camera is responding to remote controller commands
- check that everyone is prepared and wearing safety glasses
- turn on UAV lights and turn off cap lamps
- start UAV video
- fly/perform tests
- land on landing pad, if possible
- end video
- turn off UAV lights and remove light battery
- check playback to ensure control points were collected via video
- turn off and remove UAV battery (placing it in a fire-proof battery box)
- turn off remote controller
- pick up any trash off the ground (possibly broken propellers)
- take camera off UAV and put in camera box
- take props off UAV
- put UAV away and any other items left out including landing pad
- disassemble the total station if it hasn't been done already
- load total station, UAV and accessory box, paintball gun, and tripod into buggy
- ensure area is how it was (or safer) than it was upon arrival
- get in the buggy (buckled) and return to surface
- unload gear from buggy and put it back into the truck at the portal
- tag-out and sign out
- return to office on mine site
- get coordinates of measured paintball points off UAV
- return all items to GSM that belong to them (equipment and PPE)
- thank GSM and Redpath employees
- load items back into Tech vehicle, buckle up, leave site
- upload videos to Sharepoint folder
- write summary of flight and upload it to Sharepoint folder

12. Appendix C: Workflow and Procedures

This appendix contains details on the software specifications needed for successfully building 3D photogrammetry models. ADAM Technology and Bentley ContextCapture have similar 3D model construction methods, however they differ slightly. The workflow for each software is also provided.

12.1. ADAM Technology Software

The ADAM Technology software suite was developed in 1995 (ADAM Technology, 2018) and was originally designed to be optimized for creating very accurate models from a minimal set of terrestrial photos taken from preferred locations (ADAM Technology, 2010). To create a model, it is recommended to have a lens calibration file for the associated camera and lens with which the project imagery is taken. A lens calibration is created by performing a relative interior orientation with a group of photos that overlap. It is preferable that the images used for calibration be captured at a distance away from the area being captured that is similar to that of the project. Also, varying depth is also desirable for calibrations. A set of 12 overlapping photos from one of the GSM flights (the stope flight) was used for the camera lens calibration. Calibrating the lens helped to better define the interior orientation of the camera reduced distortion that the lens imposes on the imagery. The general workflow for a camera calibration in CalibCam is outlined in Figure 28. The steps calling for control data are not necessary for a camera calibration. Control data were not used for calibrating the Zenmuse X3 camera for the underground flights.

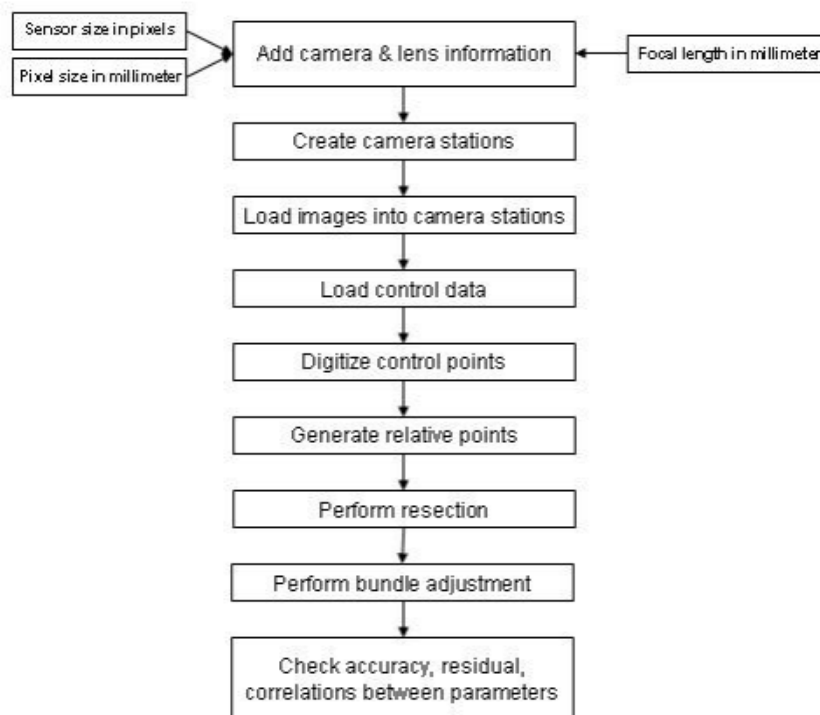


Figure 28. General workflow for 3DM CalibCam project (Lingen, 2011).

For photogrammetry projects ADAM Technology's 3DM CalibCam requires an overlap between stereopairs of 60-80% (ADAM Technology, 2010). The lens calibration is used to create a model. The steps taken to construct the model are the same steps as for the calibration, seen in Figure 28. Then, 3DM Analyst is used to map 3D structures on the merged model. Within 3DM Analyst, a stereonet can be used for data visualization and manipulation. Additionally, multiple file formats are able to be imported into 3DM Analyst for mapping.

12.2. Bentley ContextCapture Software

Bentley's ContextCapture is a newer photogrammetry software than ADAM Technology. It does not require a camera calibration, but an aerotriangulation must be performed using the model imagery (Bentley, 2018). The aerotriangulation for ContextCapture requires, the camera sensor size and the lens size, to be defined before any processing as well as locating of control

points. The control point coordinates are entered into the software and the user manually selects the control points, when visible, in each image. It should be noted that all video imagery was extracted into still images using ContextCapture. Also, ContextCapture requires approximately 50-80% overlap in between images for 3D model construction. The general workflow for Bentley ContextCapture is shown in Figure 29.

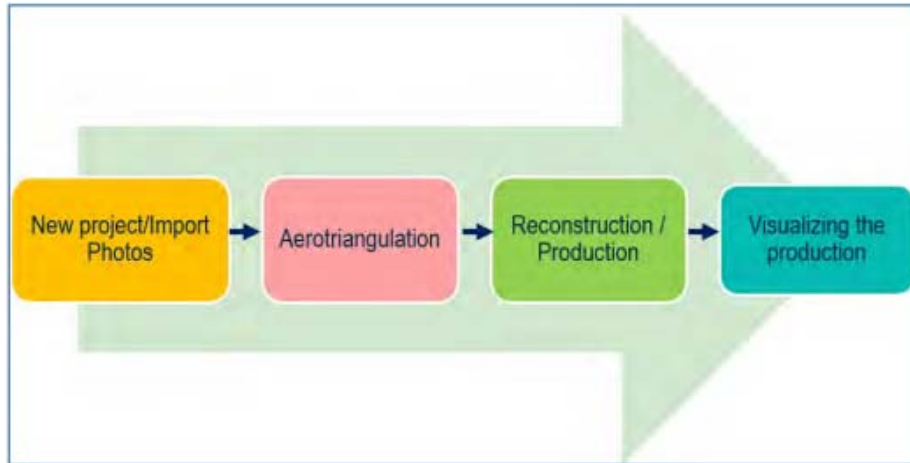
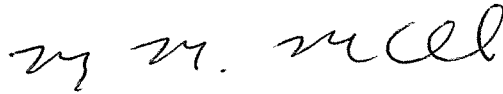


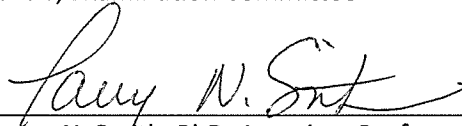
Figure 29. General workflow for constructing a photogrammetry model in Bentley ContextCapture (Bentley, 2018).

SIGNATURE PAGE

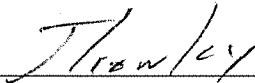
This is to certify that the thesis prepared by Elizabeth Anne Russell entitled "UAV-based geotechnical modeling and mapping of an inaccessible underground site" has been examined and approved for acceptance by the Department of Geological Engineering, Montana Tech of The University of Montana, on this 4th day of May, 2018.



Mary MacLaughlin, PhD, Professor
Department of Geological Engineering
Chair, Examination Committee



Larry N. Smith, PhD, Associate Professor and Department Head
Department of Geological Engineering
Member, Examination Committee



Jeremy Crowley, MS, Hydrogeologist and Assistant Research
Professor
Montana Bureau of Mines and Geology
Member, Examination Committee